Fall 12-2021

Hydrothermal Processes for Extraction and Conversion of Biomass to Produce Biofuels and Value-Added Products

Anuj Hemant Thakkar
Old Dominion University, anujthakkar30@gmail.com

HYDROTHERMAL PROCESSES FOR EXTRACTION AND CONVERSION OF BIOMASS TO PRODUCE BIOFUELS AND VALUE-ADDED PRODUCTS

by

Anuj Hemant Thakkar
B.S. July 2012, University of Pune, India
M.S. July 2014, Manipal University, India

A Dissertation Submitted to the Faculty of
Old Dominion University in Partial Fulfillment of the
Requirements for the Degree of

DOCTOR OF PHILOSOPHY

CIVIL AND ENVIRONMENTAL ENGINEERING

OLD DOMINION UNIVERSITY
December 2021

Approved by:

Sandeep Kumar (Director)

Xixi Wang (Member)

Mujde Erten-Unal (Member)

James W. Lee (Member)

Ayala Orlando (Member)

ABSTRACT

HYDROTHERMAL PROCESSES FOR EXTRACTION AND CONVERSION OF BIOMASS TO PRODUCE BIOFUELS AND VALUE-ADDED PRODUCTS

Anuj Hemant Thakkar
Old Dominion University, 2021
Director: Dr. Sandeep Kumar

An integrated biorefinery approach based on subcritical hydrothermal processes was developed to maximize utilization of biomass components by producing multiple products. Biomass from various sources like agricultural waste (lignocellulose), food waste (spent yeast), and dedicated cultivation (micro-algae) was used in this research.

Corn stover (agricultural waste) was hydrothermally pretreated to remove lignin and xylan while preserving most of the glucan. The pretreated corn stover was utilized to produce levulinic acid (thermochemically) and fermentable sugars (biochemically). The solid residue generated during levulinic acid production was utilized to produce biocarbon electrode material. The results generated from the experiments were used for designing a pilot facility to process one ton of corn stover per day.

A continuous-flow hydrothermal treatment 'flash hydrolysis' was deployed for yeast protein recovery. The liquid hydrolysate with the solubilized amino acids and peptides was tested as nutrient for cultivation of *E. coli* in a continuous bioreactor and the yields were compared with the commercial yeast extract. Finally, the kinetic parameters for yeast solubilization like reaction order, activation energy, and pre-exponential factor were determined.

High-protein micro-algae (*Scenedesmus sp.*) slurry was parallelly fractionated using flash (continuous mode) and acid (batch mode) hydrolysis. Most of the proteins and carbohydrates in micro-algae were recovered in liquid hydrolysate whereas the lipids in solid residue were

extracted using organic solvent. The flash and acid hydrolysis derived post extraction solid residue was thermally activated to produce highly porous biocarbon nanosheets.

Overall, the developed processes provide multiple value-added products generated from renewable sources for a greater financial and environmental sustainability. Also, strategies to improve and down select the developed technologies were discussed.

This dissertation is dedicated to my family. Starting with the youngest member, my little niece Mahee, who put a smile on my face during good and bad days. I can't thank my wife Ekta enough for sacrificing so much so that I could pursue my dreams. My loving sister Meghna and brother-in-law Anand have always been there for me throughout the doctorate program. I dedicate this work to my parents, Hansa and Hemant Thakkar, for believing in my abilities and encouraging me to achieve greater heights every day.

ACKNOWLEDGMENTS

I wish to express my sincere appreciation and gratitude to my principal advisor, Dr. Sandeep Kumar, for his guidance, encouragement, and support. I am also very grateful to my committee members, Dr. Xixi Wang, Dr. Mujde Erten-Unal, Dr. James W. Lee, and Dr. Ayala Orlando for their valuable feedbacks. I would like to acknowledge the Department of Civil and Environmental Engineering (CEE) and the very well-equipped Biomass Research Laboratory (BRL) for providing the platform for my research work. A special thanks to Dr. Ishibashi Isao for directing this graduate program. I would like to mention CEE office staff, Melanie Agustin and Sara Champlin, for their administration and timely help. I am forever grateful to all the past and present students working in the BRL for their friendship, collaboration, and trainings. Again, I thank Dr. Sandeep Kumar for his untiring efforts to acquire research grants and funding my research. I would like to acknowledge Department of Energy (DOE), National Renewable Energy Laboratory (NREL), and Sandia National Laboratories (SNL) for the financial support.

NOMENCLATURE

AC	Activated Carbon
AH	Acid Hydrolysis
ALU	Algal Lipid Upgrading
ATCC	American Type Culture Collection
BET	Brunauer, Emmett, and Teller
BPR	Back Pressure Regulator
C	Carbon
C_2H_5OH	Ethanol
CH_4	Methane
CO_2	Carbon Dioxide
CSTR	Continuous Stirred-Tank Reactor
DI	Deionized Water
DOE	Department of Energy
DW	Dry Weight
EA	Elemental Analyzer
EPA	Environmental Protection Agency
FAME	Fatty Acid Methyl Esters
FAO	Food and Agricultural Organization
$FeCl_3$	Ferric Chloride
FH	Flash Hydrolysis
FTIR	Fourier-Transform Infrared Spectroscopy
GABA	Gamma-Aminobutyric Acid
GHG	Greenhouse Gas
GRAS	Generally Recognized as Safe
HCl	Hydrochloric Acid
HMF	Hydroxymethyl Furfural
HPLC	High Pressure Liquid Chromatography
HTC	Hydrothermal Carbonization
HTL	Hydrothermal Liquefaction
IBR	Integrated Biorefinery
IC	Ion Chromatography
ID	Internal Diameter
IR	Impregnation Ratio
K_2CO_3	Potassium Carbonate
KOH	Potassium Hydroxide

LA	Levulinic Acid
LAP	Laboratory Analytical Procedures
LB	Lysogeny Broth
LCA	Life Cycle Assessment
MCE	Mixed Cellulose Ester
MSW	Municipal Solid Waste
MUFA	Monounsaturated Fatty Acid
N	Nitrogen
NaOH	Sodium Hydroxide
NREL	National Renewable Energy Laboratory
O	Oxygen
P&ID	Process & Instrumentation Diagram
PCS	Pretreated Corn Stover
PESR	Post-Extraction Solid Residue
PFD	Process Flow Diagram
PFR	Plug Flow Reactor
RI	Refractive Index
PPE	Personal Protective Equipment
PUFA	Polyunsaturated Fatty Acid
QSDFT	Quenched Solid Density Functional Theory
RCS	Raw Corn Stover
RNA	Ribonucleic Acid
SEM	Scanning Electron Microscope
SFA	Saturated Fatty Acid
SNL	Sandia National Laboratories
SSE	Sum of Squares Error
TEA	Techno-Economic Analysis
TEM	Transmission Electron Microscope
TGA	Thermogravimetric Analyzer
TN	Total Nitrogen
TOC	Total Organic Carbon
UHS	Unhydrolyzed Solids
XRD	X-Ray Diffraction
YE	Yeast Extract
$ZnCl_2$	Zinc Chloride

TABLE OF CONTENTS

Page

LIST OF TABLES

LIST OF FIGURES

CHAPTER 1

INTRODUCTION

Note: Some contents of this chapter were adapted from the chapters published in the book 'Sub- and Supercritical Hydrothermal Technology'.

A. Thakkar, S. Kumar, Supercritical Water Gasification of Biomass: Technology and Challenges, in: Sub-and Supercrit. Hydrothermal Technol., CRC Press, 2019: pp. 85–105.

A. Thakkar, S. Kumar, Hydrothermal Carbonization for Producing Carbon Materials, in: Sub- and Supercrit. Hydrothermal Technol., CRC Press, 2019: pp. 67–83.

A growing interest in research involving renewable energy and materials has been observed in the last few decades, due to finite reserves of fossil fuels and the environmental concerns, specifically global warming. United Nations has quoted that climate change is a defining issue of our times, and we are currently at a defining moment. At this point of time, the world heavily relies on the fossil fuels for its energy demand. As per the 'Renewables 2020 Global Status Report', in 2018 the share of fossil fuels and modern renewables in final energy demand was 79.9% and 11%, respectively [1]. Various renewable options currently being explored and utilized are wind, hydro/oceanic, geothermal, solar, and biomass energies. Among all these options, biomass is the only renewable source capable of directly producing solid, liquid, and gaseous fuels. Other than bioenergy, biomass can also be used to produce renewable biochemicals.

Biorefineries are being developed to utilize biomass to produce bioenergy and value-added products, based on the concept of today's petroleum refinery. Biorefinery involves a sequence of environmentally friendly processes that employs biomass as raw material [2–4]. Biofuels have been explored as an alternative to reduce the dependence on petroleum. Biofuels are obtained from biomass through chemical, physical, or biological processes. They present several advantages such as easy availability, clean processing, and biodegradability. Overall,

utilization of biomass for the production of fuel and chemicals is considered as a potential sustainable solution for modern needs.

Greenhouse gas (GHG) emissions from the use of fossil fuels can be mitigated up to a certain extent by replacing it with biofuels produced from biomass [5]. Photosynthetic biomass is seen as power banks of solar energy, its additional advantage is in its wider distribution in the world which may eliminate the regional dependence for the energy sources. Energy security along with environmental concerns have also made scientists around the world tap the potential of biomass as an alternative raw material. It is a sustainable source of energy that can also help in regional economic development. Currently, it is the fourth largest source of energy for the world and is projected to contribute 10–20 % of total energy by the end of the 21st century [5].

1.1 Classification of Biomass

Two major biofuel production pathways that are commercialized so far are fermentation of sugars to produce ethanol and transesterification of oils obtained to produce biodiesel. Sugars used for ethanol production are extracted from crops like corn and sugarcane. Ethanol has a high octane number (108) and has the advantage of being able to be used in automobile engines [6]. On the other hand, biodiesel is produced from oils extracted from oilseeds like canola, jatropha etc. The downside of these two technologies is that it requires fertile land and water for the cultivation of feedstock and thus raises the issue of ‘food vs. fuel’. This issue makes it necessary to explore biomass sources that do not compete with food crops for cultivation land and water. Various kinds of biomass like agricultural waste, food waste, and micro-algae are being used to produce valuables employing environment friendly processes.

1.1.1 Agricultural Waste

Lignocellulose in form of agricultural, forest, and industrial residues makes almost 90% of available land biomass. Lignocellulosic agricultural waste is plant cell wall construction material which is abundantly available and does not directly compete with food and feed production [7]. Dedicated energy crops, such as switchgrass and poplar, are also being grown to meet energy demands, however, these crops compete with food and feed production. Lignocellulosic biomass is made up of four major components: cellulose, hemicellulose, lignin, and ash. The proportion of each of these components varies with the kind of biomass and many other factors. Lignocellulosic material is a promising feedstock for the production of bioethanol and other biochemicals [8].

Agricultural residues such as corn stover, wheat straw, rice straw, bagasse, and wheat bran are rich in lignocellulose. Corn stover is the residue after harvesting corn kernel which comprises of stalks, leaves, cobs, and husks [8]. In the United States alone, more than 100 million dry tons of corn stover is produced per annum [9]. It has many potential applications, and a few are discussed in greater detail in Chapter 2.

1.1.2 Food Waste

Municipal solid waste (MSW) is a complex mixture, typically consisting of food waste, glass, metals, yard trimmings, woody waste materials, non-recyclable paper and plastic, construction and demolition waste, rags, and sludge from wastewater treatment. The composition and classification of MSW varies substantially between different municipalities worldwide. Although it consists of both biodegradable and non-biodegradable fractions from organic and inorganic materials, respectively. Using MSW as a feedstock for energy is a challenge due to its low energy content, high moisture, heterogeneous composition, and distributed availability.

Organic food waste is one of the major MSW contributors. About 20 million tons of CO_2 equivalent greenhouse gases (GHG) is emitted due to food waste every year. As per Food and Agricultural Organization (FAO), globally every year about $750 billion worth of food waste is generated. One-third of total food produced for humans is wasted, which is approximately 1.6 billion tons per year. 54% of this food is wasted during production, post-harvest handling, and storage. Whereas the rest is wasted when it enters into the processing industry [10,11]. Incineration and landfills are most widely used food disposal techniques. Incineration causes the release of pollutants like dioxins, furans, and particulates while landfills lead to issues like odor, pests, and GHG emission [12,13]. Food wastes have considerable amount of water/moisture in it which makes incineration a poor disposal choice. Various food wastes generated like fruits, vegetables, sugarcane bagasse, food processing industry by-products, etc., can be used as feedstock for producing energy and biochemicals. In this research work (Chapter 3), a process was developed to utilize spent yeast which is generated as waste during fermentation process in the food and beverage industry.

1.1.3 Micro-algae

Micro-algae can be grown in marine and freshwater in the presence of CO_2 and sunlight through photosynthesis. The biomass productivity of micro-algae is much higher than other photosynthetic terrestrial plants. Also, unlike dedicated energy crops, micro-algae do not occupy fertile land meant for growing food crops [14–16]. The productivity of micro-algae can be 50 times higher than that of dedicated energy crops like switchgrass [17]. Out of more than 50,000 algae species present on earth, very few are studied and utilized for various applications. Algal cells are made up of proteins, carbohydrates, lipids, and ash in different proportions specific to the species and growth conditions. Uniform transportation of highly concentrated micro-algae

solution into and out of the reactor is easier owing to its density and other physical properties compared to lignocellulosic biomass [18]. Algae can be converted into bio-crude through hydrothermal liquefaction (HTL) which also generates gaseous phase, solid residue, and carbon-rich aqueous phase. The fraction of biomass in the aqueous phase is generally in the range of 30–50% and can be as high as 68% [19]. Micro-algae species with higher lipid content are suitable feedstock for the production of renewable energy (biofuels) and those with higher protein and carbohydrate are ideal for producing food supplements, human nutritional products, cosmetics, and animal feed [20].

1.2 Biomass Processing Technologies

Chemical processes that are safe and environment friendly have been increasingly talked about in recent times. To have green chemical processes at commercial scale, the change should be brought in through research and development. There are multiple technologies for conversion of biomass to biofuels and biochemicals. Basically, the technologies can be divided into two main categories, biochemical and thermochemical [21]. Processes that utilize micro-organisms and enzymes are classified under biochemical processes; whereas, processes like combustion, gasification, pyrolysis and hydrothermal technology that utilize high temperature come under thermochemical processes. In the case of bioethanol production from lignocellulosic biomass, a sequential combination of thermochemical (pretreatment) and biochemical (enzymatic hydrolysis and fermentation) process is also employed [6]. This research work is mainly based on hydrothermal technology (thermochemical process), but it also utilizes enzymatic hydrolysis (biochemical process) in small extent. The details of these two processes are discussed further in this chapter.

1.2.1 Enzymatic Hydrolysis (Biochemical Process)

A class of enzymes called cellulases are used to breakdown cellulose to glucose which is further fermented to ethanol. High cost of cellulases is a challenge in enzymatic hydrolysis of lignocellulosic materials for bioethanol production. Cellulases are produced via fermentation using mainly fungi and bacteria. Fungi is preferred over bacteria due to their permeation capability and versatile substrate consumption. Enzymatic hydrolysis of lignocellulosic biomass has some limitations which prevent the process to be economically feasible. To overcome these limitations, various strategies are implemented including genetic engineering, enzyme recycling, high solid loadings, pretreatment technologies, supplementation of cellulases with additives, and application of nanomaterials for improving the thermal and pH stability of cellulases. Bioreactors are used for efficient biomass hydrolysis to produce fermentable sugars. The key factors for designing a bioreactor include efficient mixing, sufficient mass transfer, low shear stress, low foaming problems, and low consumption of water and energy [22].

1.2.2 Hydrothermal Technology (Thermochemical Process)

Since most of the biomass from various sources have significant amount of moisture, conversion processes like hydrothermal that do not require drying, or dewatering have an advantage. For example, in case of micro-algae biorefineries, techno-economic and lifecycle analysis suggest that dewatering stage is one of the most energy intensive process [23,24]. Other thermochemical processes like pyrolysis, require dry biomass whereas thermal gasification generally requires biomass with less than 10% moisture [25].

In the 1900s, organic solvent substitution was promoted as one of the methods to make chemical processes environmentally friendly and reducing the amount of hazardous wastes [26]. When water is heated under sufficient pressure to maintain its liquid or supercritical state, it is

called as sub or supercritical water. It is considered as one of the most promising mediums or reactants for replacement of organic solvents. Hydrothermal (sub and supercritical water) technology can be integrated in industrial processing for safer, more flexible, economical, green, and sustainable engineering [27].

The properties of water at various temperature and pressure conditions are shown in Table 1. The enhanced transportation and solubilization properties of sub and supercritical water play an important role in the transformation of biomass to high energy density fuels and functional materials [28]. Sub and supercritical water help in performing hydrolysis, depolymerization, dehydration, and decarboxylation reactions. The proton-catalyzed mechanism, direct nucleophilic attack mechanism, hydroxide ion catalyzed mechanism, and the radical mechanism play important roles in the conversion of biomass in hydrothermal medium [29,30].

Water above its boiling temperature (100 °C) and below its critical temperature (374 °C) under adequate pressure that is more than the vapor pressure at that point is called subcritical water. Subcritical water has a wide range of applications like extraction, liquefaction, carbonization, gasification, coolant in nuclear power plants, aqua-thermolysis, waste oxidation, inorganic synthesis, and mineralization. Some of these technologies have already matured and are on the cusp of commercialization [27]. Water heated above 374 °C and pressurized beyond 22.1 MPa possesses unique physical and chemical properties and is known as supercritical water. At supercritical conditions, water behaves like a nonpolar solvent and thus solvates organic molecules. Supercritical water has some of the desired properties of its liquid phase as well as the gaseous phase. The properties of water above critical point enhance reaction kinetics along with the rise in diffusivity and free radical reactions. However, these changes in the property of

water above critical point move the reaction toward gas formation rather than solid or liquid products.

Table 1. Properties of water at various conditions [31,32]

	Normal water	**Subcritical water**		**Supercritical water**	
Temperature (°C)	25	250	350	400	400
Pressure (MPa)	0.1	5	25	25	50
Density, ρ (g/cm^3)	1	0.8	0.6	0.17	0.58
Dielectric constant, ε (F/m)	78.5	27.1	14.07	5.9	10.5
Ionic product, pKw	14	11.2	12	19.4	11.9
Heat capacity, Cp (KJ/Kg/K)	4.22	4.86	10.1	13	6.8
Dynamic viscosity, η (mPa s)	0.89	0.11	0.064	0.03	0.07

Hydrothermal treatment of biomass can also be broadly classified into three different processes; liquefaction, catalytic gasification, and high-temperature gasification based on the final product and reaction condition. Reaction temperature in the range of 200-370 °C is used when biomass is to be liquified into bio-oil/bio-crude. Whereas temperature in the range of 374–550 °C is used for hydrothermal gasification in the presence of catalyst to enhance reaction efficiency, reaction rates, and selectivity. At relatively higher temperature (550–700 °C),

gasification can be done without use of a catalyst or by using activated carbon or alkali catalyst to inhibit tar formation [33–35]. Other than these three major processes, subcritical water in the range of 150-300 °C can be also effectively used for pretreatment, hydrolysis, and extraction of components from biomass feedstocks by controlling the reaction time. Most of the research work in this dissertation was done using these conditions.

1.3 Research Intent

In this research, biomass from various sources like agricultural waste (lignocellulose), food waste (spent yeast), and dedicated cultivation (micro-algae) was utilized. The objective of this research was to develop and design biomass conversion or solubilization processes that result in minimal waste, high energy efficiency, low toxicity, cost-effectiveness, and minimal impact over life cycle. Biorefineries are being developed globally, however, developing an economically viable process is still a challenge. An integrated biorefinery concept is a novel and economical process intensification methodology which maximizes utilization of biomass components by producing multiple products from various streams generated while processing the feedstock. This research focuses on the application of subcritical hydrothermal processes for producing biofuel precursors and biochemicals from biomass via an integrated approach. The summary of this research work is shown in Fig. 1.

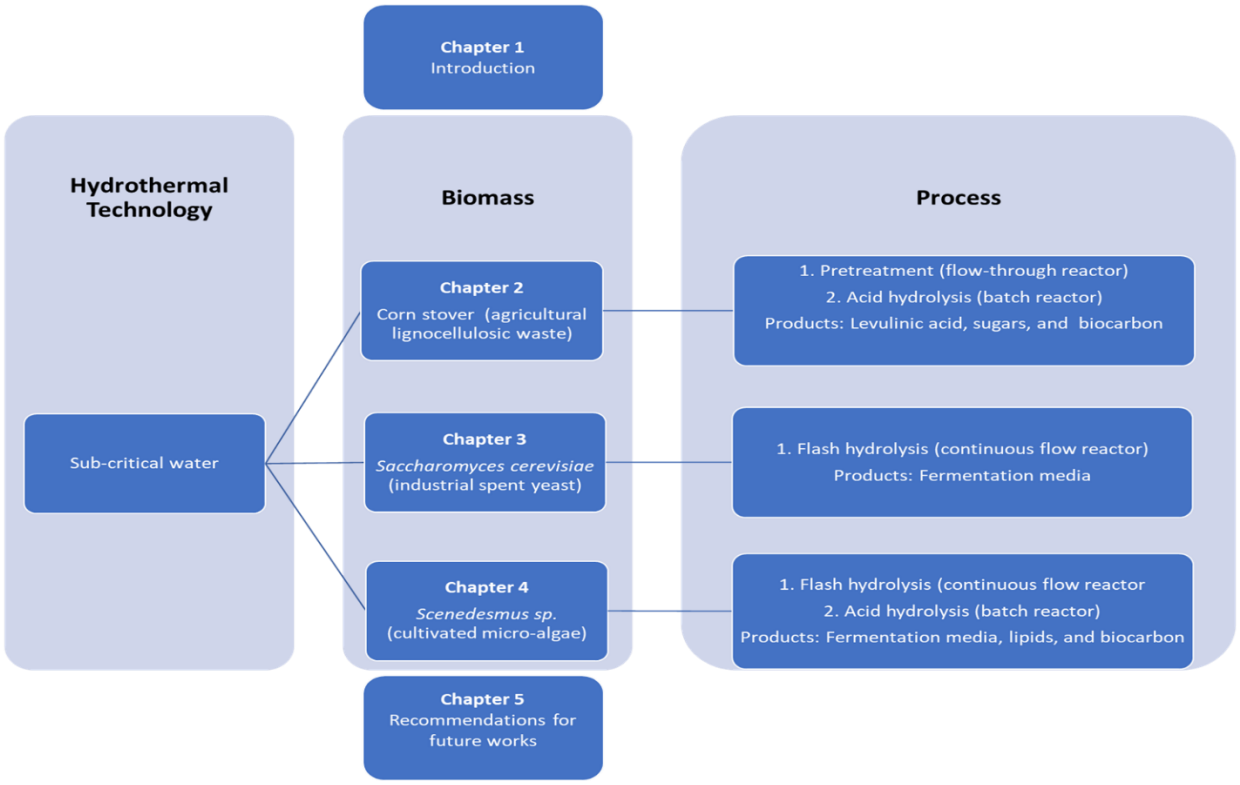

Figure 1. The summary of this research work

CHAPTER 2

DEVELOPMENT OF AN INTEGRATED BIOREFINERY PROCESS USING CORN STOVER TO PRODUCE MULTIPLE BIOCHEMICALS

Note: The contents of this chapter were adapted from the research article published in the journal 'Fuel Processing Technology'.

A. Thakkar, K.M. Shell, M. Bertosin, D.D. Rodene, V. Amar, A. Bertucco, R.B. Gupta, R. Shende, S. Kumar, Production of levulinic acid and biocarbon electrode material from corn stover through an integrated biorefinery process, Fuel Process. Technol. (2020) 106644.

To overcome the inefficient biomass conversion, waste generation, and lack of co-production in biorefineries, an integrated process was proposed for the conversion of corn stover into levulinic acid, fermentable sugars, and biocarbon electrode material. Corn stover was pretreated through hydrothermal process using 0.45 wt.% K_2CO_3 which removed 76 wt.% lignin and 85 wt.% xylan while preserving 83 wt.% glucan. This was followed by acid hydrolysis to produce levulinic acid at varying H_2SO_4 concentrations and reaction time in a batch reactor at 190 ℃. At a reaction time of 5 min in 2 wt.% H_2SO_4, 35.8 wt.% and 30 wt.% glucan in raw and pretreated corn stover was converted to levulinic acid, respectively. The residue from acid hydrolysis was converted into biocarbon for supercapacitor electrodes via a two-step thermal activation process which showed a specific capacitance of 120 F g^{-1}. The details related to the biocarbon electrode production other than the properties of final product were excluded from this chapter since this part of the research was done by a collaborator. A biochemical (enzymatic) conversion pathway to produce fermentable sugars from pretreated corn stover which is an alternative to the thermochemical (acid hydrolysis) pathway to produce levulinic acid was also experimented. The enzymatic glucan digestibility of raw and pretreated corn stover was found to be 19% and 93%, respectively. The proposed integrated biorefinery concept provides multiple value-added products for a greater financial and environmental sustainability.

2.1 Introduction

Despite the growing interest in bioeconomy and renewables, the biorefinery industry has struggled to achieve economic competitiveness. Some of the major bottlenecks biorefineries encounter are inefficient biomass conversion processes, waste generation, and lack of processes for co-production of value-added compounds [36,37]. To overcome these challenges, advanced approaches include integration of biofuel production with other products, which use biomass or process residues to make different co-products like biofuel, bio-chemicals, fertilizer, heat, energy, etc. [38].

Corn stover is recognized as an important agricultural waste with many potential applications in growing bioeconomy [39]. It is estimated that more than 100 million dry tons per annum of corn stover is produced in the USA alone [40]. The chemical composition of various lignocellulosic biomass differs considerably and is influenced by genetic and environmental factors [41]. Lignocellulosic biomass like corn stover is composed of cellulose, hemicellulose, and lignin [42,43].

National Renewable Energy Laboratory (Denver, USA) reported levulinic acid as one of the top value-added chemicals produced from biomass. Levulinic acid is a member of the gamma-keto acid group which can be produced through acid-catalyzed dehydration and hydrolysis of hexose sugars [44–46]. The most widely used method for levulinic acid production is acid catalyzed single step reaction without removing hemicellulose and lignin from the lignocellulosic biomass [47–50]. Due to formation of byproduct formic acid, the theoretical yield of levulinic acid from hexose is only 64.5 wt.%. Practically, the yield is even lower due undesired side reactions [51]. The acidic conditions also hydrolyze and hydrate pentoses in hemicellulose to furfural, which at harsher condition, undergo further degradation [52]. One of

the major drawbacks of the lignocellulosic biomass to levulinic acid conversion process is unavoidable formation of solid byproduct [53,54], which is formed due to the decomposition of lignin, cellulose, and hemicellulose during acid catalyzed reactions to form intermediate that re-polymerize to insoluble material termed humins [44].

The loss of hemicellulose and lignin to the degraded products can be reduced by carrying out the conversion into two separate steps, where the first step removes components other than cellulose from the biomass. These recovered hemicellulose and lignin derived components can be used to produce furfural [52], carbon microspheres [42], levulinic acid [55], and other biobased materials using suitable reaction conditions [46]. The most common first step pretreatment process for the production of levulinic acid from biomass uses acidic conditions which sufficiently removes hemicellulose but not lignin [52,56–58]. Disposal issues and higher costs associated with the use of acids and alkalis for pretreatment also bring in additional economic and environmental challenges [59–62].

The first step using moderate alkaline hydrothermal condition has potential to pretreat biomass efficiently and economically. Hydrothermal reactions use water as reaction media which is environmentally benign and inexpensive. If not regulated, the pH of the hydrolysate produced during hydrothermal pretreatment decreases due to formation of organic acids. The use of potassium carbonate (K_2CO_3) to regulate pH of the reaction media is advantageous compared to pretreatment using acidic catalyst as there is no cost associated with acid recovery and handling [42]. The pH range of 4–7 and a flow through reactor setup (described in section 2.2.1), minimizes the formation of degradation products that can catalyze hydrolysis of the cellulosic material during pretreatment [63–69]. The reactive and soluble lignin fractions need to be rapidly removed from the system before they recondense and become part of biomass solid [70,71].

Liquid hydrolysate generated from the pretreatment of lignocellulosic biomass using K_2CO_3 in a flow through reactor, contains 25–45% of the initial biomass carbon, mostly in the form of sugars from hemicelluloses, degradation products such as furfural, lignin derived phenolic compounds, and carboxylic acids [42].

In addition, literature suggests biomass is an excellent precursor material for energy storage devices, such as supercapacitors. In supercapacitors, the energy storage mechanism is created from an applied voltage, whereby ions are stored electrostatically on the surface and within the pores of the material [72]. Currently, carbons from petroleum coking processes are utilized in the commercial production of supercapacitors, generating a need for more sustainable approaches for supercapacitor fabrication [73]. Biomass is an excellent alternative electrode material due to its renewability, abundance, and the potential for high surface areas post activation. Corn derived biocarbons for energy storage applications has been previously reported with capacitances reaching higher than 300 F g^{-1}, with chemical or catalytic activation techniques [74–78]. However, the use of solid waste streams from the production of biofuel precursors in energy storage devices is a novel idea within the field of biomass derived energy storage devices.

The biochemical (enzymatic) conversion pathway to produce fermentable sugars from pretreated corn stover is an alternative to the thermochemical pathway to produce levulinic acid. The fermentation of these sugars to ethanol is one of the most promising technologies for large scale bioethanol production. The efficiency of the enzymatic hydrolysis process is based on the effectiveness of the pretreatment step. Hydrothermal alkaline pretreatment removes lignin and hemicelluloses from the biomass which changes its surface area, crystallinity, pore size distribution, and degree of polymerization. These changes help in improving accessibility of β-glycosidic linkages to cellulase enzymes. Nevertheless, selecting an appropriate pretreatment

process is critical because it is one of the most expensive steps in conversion of lignocellulosic biomass to bioethanol and may account for up to 40% of the processing cost [42].

In this work, the hydrothermal pretreatment (i.e., the first step) of corn stover was conducted in a flow through reactor using K_2CO_3 solution followed by batch acid hydrolysis (i.e., the second step) of pretreated biomass to produce levulinic acid using sulfuric acid (H_2SO_4). The solid residue produced during the acid hydrolysis (i.e., the second step) was used as a starting material for the synthesis of electrode material for energy storage applications such as batteries and supercapacitors. As an alternative to acid hydrolysis, enzymatic hydrolysis of pretreated corn stover was also experimented to evaluate the parameters for designing a pilot facility to process one ton of corn stover per day.

2.2 Material and Methods

Potassium carbonate (K_2CO_3), sulfuric acid (H_2SO_4), hydrochloric acid (HCl), ethanol (C_2H_5OH), and analytical grade standards were purchased from Fisher Scientific. Cellulase enzyme blend 'Cellic CTec2' was purchased from Sigma-Aldrich. De-ionized water was used for all the experiments unless otherwise specified.

2.2.1 Hydrothermal Pretreatment of Biomass

The experimental setup and protocol for hydrothermal pretreatment were similar to the one used by Kumar et al. [42]. The reactor system consists of high-pressure pump, electrical tubular furnace, tubular reactor, heat exchanger, and backpressure regulator. The reactor was a 9/16'' (14.28 mm) ID and 65 ml volume high-pressure stainless-steel tube. Temperature of the reaction zone was measured using a 1/16'' (1.58 mm) thermocouple placed inside the biomass bed from the inlet. Real time temperature indicated by the thermocouple was recorded at an

interval of 5 min during the pretreatment. Reactor pressure was maintained using a backpressure regulator and a pressure gauge.

The 10% and 90% cumulative particle passing sieve sizes for the milled corn stover provided by the Idaho National Laboratory were 0.23 and 2.68 mm, respectively. The reactor was placed inside the preheated furnace after packing with 11 g of corn stover. A stainless-steel frit of 2 mm pore size was placed at the reactor outlet to restrict the biomass in the reactor. The experiment was divided into three phases of 20 min each based on the temperature, heating (25–190 ℃), reaction (190 ℃), and cooling (190–50 ℃). 0.45 wt.% K_2CO_3 solution was pumped into the reactor using the high-pressure pump. The flow rate of 2.5 ml/min was maintained during heating and reaction phase and 9.9 ml/min during cooling phase. Constant reaction pressure of 3.44+/-0.15 MPa, which is higher than the vapor pressure of water in the temperature range of study was maintained throughout to keep the water in the K_2CO_3 solution in liquid phase. Liquid hydrolysate was continuously collected at the outlet of the reactor for all three phases, pH was measured. Utilization of liquid hydrolysate generated during hydrothermal pretreatment of corn stover to produce value-added products from solubilized lignin and hemicellulose is being studied currently and is beyond the scope of this manuscript. The gaseous products which were appreciably low in the temperature range of study were vented without analysis. Total organic carbon (TOC) content in hydrolysate was analyzed using Shimadzu TOC/TN analyzer. Raw and pretreated corn stover were analyzed for biochemical and elemental composition. Biochemical composition analysis was based on the NREL/TP-510-42618 standard procedure [79]. High pressure liquid chromatography (HPLC) with Bio-Rad Aminex HPX-87P column was employed for determination of sugars. Elemental composition (Carbon, Hydrogen,

Nitrogen, and Sulfur) was analyzed using Flash 2000 Elemental Analyzer by Thermo Scientific using a 2,5-Bis(5-tert-butyl-benzoxazol-2-yl)thiophene standard for calibration.

2.2.2 Acid Hydrolysis of Biomass for Levulinic Acid Production

The experimental setup for acid (H_2SO_4) hydrolysis of biomass consisted of a tubular reactor and sand-bath heater. The 54.2 ml stainless-steel tubular reactor was sealed with 1/16'' (1.58 mm) thermocouple on one end and a cap on the other. Real time temperature indicated by the thermocouple was recorded continuously during the reaction. In a typical reaction, the reactor was placed in the preheated sand-bath at 200 ℃. The reactor took 15 min to reach desired reaction temperature of 190 ℃. The reaction was carried out for varied reaction time at 190 ℃ and then quenched to 30 ℃ instantaneously using a cold-water bath. The volume of the water or acid solution used for all the reactions was 47.6 ml, chosen such that upon heating to the desired temperature, the autogenous pressure buildup maintains the water in liquid phase. The biomass loaded in the reactor was 0.95 g, which was 2 wt.% of the reaction medium. After the reaction, liquid hydrolysate and solid residue were separated by centrifuging the reaction mixture at 8000 rpm. TOC content in hydrolysate was analyzed using Shimadzu TOC/TN analyzer. HPLC with Bio-Rad Aminex HPX-87H column was used for quantification of organic compounds lactic acid, formic acid, acetic acid, levulinic acid, hydroxymethylfurfural (HMF), and furfural in liquid hydrolysate. The percentage contribution of carbon by these organic compounds towards the dissolved TOC was calculated based on the concentration of these compounds and their carbon content. At select reaction condition, the solid residue generated was quantified as percentage of biomass loaded and analyzed for elemental composition as mentioned in section 2.2.1. Both raw and pretreated corn stover were hydrolyzed using 0, 1, 2, and 4 wt.% H_2SO_4 and reaction time of 5 min to find the optimum H_2SO_4 concentration to produce levulinic acid. Using

optimum H_2SO_4 concentration, reaction time of 15, 45, 105, and 165 min were experimented to study its effect on the product profile. The levulinic acid yield for all the experiments was calculated using equation 1.

$$\text{Yield (\%)} = \frac{\text{Levulinic acid conc. (mg/ml)} \times \text{Vol. of hydrolysate (ml)} \times 100}{\text{Biomass loaded (mg)} \times \text{Glucan conc. in biomass (\%)}} \quad (1)$$

2.2.3 Enzymatic Hydrolysis of Biomass and Pilot Facility Design

Enzymatic hydrolysis of the raw and pretreated corn stover was carried out in 500 ml flasks sealed with rubber stoppers. Other than the scale (300 ml reaction mixture), biomass loading (3 wt.%), and enzyme loading (40 mg protein per g of glucan), all other hydrolysis conditions like temperature (50 ℃), 1 M sodium citrate buffer pH (5-5.5), and concentration of anti-microbial agent (5.0% sodium azide) were selected as per the NREL LAP 'Enzymatic saccharification of lignocellulosic biomass' [80]. Cellulase enzyme blend 'Cellic CTec2' used in this study had enzyme concentration of 376.3 mg/ml. Flasks were placed in an incubator shaker to maintain constant temperature of 50 ℃ at 150 rpm. Liquid hydrolysate was separated from the unhydrolyzed solids (UHS) after 72 h of hydrolysis and placed in boiling water for 10 min to stop the reaction. High pressure liquid chromatography (HPLC) with Bio-Rad Aminex HPX-87P column was employed for determination of released sugars in the liquid hydrolysate. The enzymatic digestibility was calculated as the ratio of glucan equivalent of glucose + cellobiose in the liquid hydrolysate to the initial glucan loading. Glucan equivalent of glucose and cellobiose was calculated as 0.9 × solubilized glucose amount + 0.95 × solubilized cellobiose amount. The UHS was washed with DI water and dried overnight at 105 ℃ to calculate the yield. Utilization of UHS generated during enzymatic hydrolysis of pretreated corn stover to produce value-added products is being studied currently and is beyond the scope of this article. The results generated

from the pretreatment and enzymatic hydrolysis experiments were used for designing a pilot facility to process one ton of corn stover per day. Process flow diagram (PFD) with material balance and process & instrumentation diagram (P&ID) were developed for hydrothermal pretreatment and enzymatic hydrolysis. This design was a part of an integrated biorefinery being developed in collaborations with other universities and research labs.

2.3 Results and Discussion

Fig. 2 depicts the proposed conversion scheme for corn stover to levulinic acid and biocarbon electrode material with detailed process insets. All experiments were performed in duplicate and the reported results are averages of two values. The deviation associated with all the results was less than 5% except for the capacitance values which deviated up to 12%.

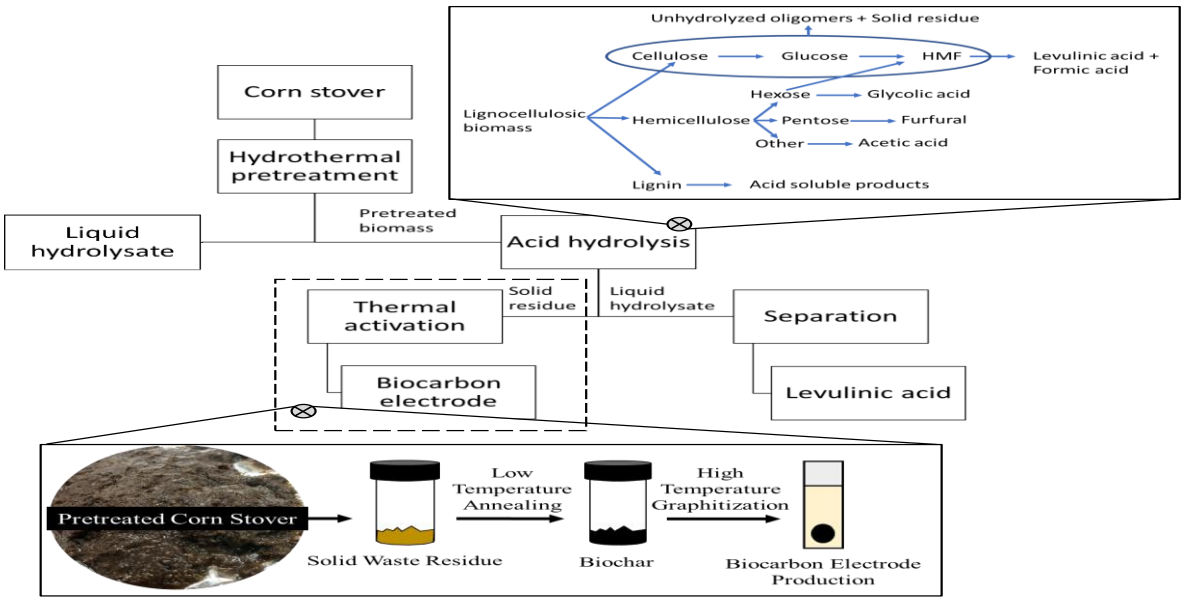

Figure 2. Proposed conversion scheme for corn stover to levulinic acid and biocarbon electrode material with detailed process insets

2.3.1 Analysis of Products from Hydrothermal Pretreatment of Biomass

The biochemical composition analysis of the raw and pretreated corn stover in wt.% is shown in Table 2. 90% of hemicellulose in raw corn stover was made up of xylan. Hydrothermal pretreatment removed 76% of lignin and 85% of xylan from raw corn stover while retaining 83% of glucan. The concentrations of galactan and mannan, if present in the biomass, were less than the detection limit of Refractive Index (RI) detector in HPLC. The concentration of arabinan was found to be 2.5% and 0.3% in raw and pretreated corn stover, respectively. The loss of biomass due to solubilization was 62.4%. Due to biomass loss, the ash content in the pretreated biomass rose to 9.4%. The pH of the liquid hydrolysate generated after pretreatment were 6.3, 4.2, and 9.5 for the heating (25–190 ℃), reaction (190 ℃), and cooling (190–50 ℃) phases, respectively. For the hydrolysate, using 0.45 wt.% K_2CO_3 helped in maintaining a pH above 4 over all three phases and thus reducing the loss of glucan to as low as 17% during the pretreatment process.

Table 2. Biochemical composition analysis of raw and pretreated corn stover

Biomass	Ash (%)	Lignin (%)	Glucan (%)	Xylan (%)	Arabinan (%)	Others (%)
Raw corn stover	6.5	27.0	28.2	21.6	2.5	14.2
Pretreated corn stover	9.4	18.0	62.0	8.7	0.3	1.6

2.3.2 Analysis of Products from Acid Hydrolysis of Biomass

The effect of H_2SO_4 concentration on levulinic acid yield was investigated, where the reaction time of 5 min was used for all the experiments. The optimum H_2SO_4 concentration for maximizing levulinic acid yield was found to be 2 wt.%, for both raw and pretreated corn stover. As shown in Fig. 3, with an increase in H_2SO_4 concentration from 0 wt.% to 2 wt.%, the yield of levulinic acid increased from less than 0.2% to 35.8% and 30% for the raw and pretreated corn stover, respectively. At 4 wt.% H_2SO_4, the yield of levulinic acid for the raw and pretreated corn stover dropped to 19.7% and 21.5%, respectively, from the maximum obtained at 2 wt.% H_2SO_4. The drop in levulinic acid yield at 4 wt.% H_2SO_4 could be due to higher degradation of cellulose, glucose, and HMF to form solid residue according to the simplified decomposition of lignocellulosic biomass shown in Fig. 2 [44]. The levulinic acid yield of 35.8% for raw corn stover and 30% for pretreated corn stover obtained using 2 wt.% H_2SO_4 is equivalent to 48 mol.% and 42 mol.%, respectively, based on moles of levulinic acid produced per mole of anhydrohexose in biomass feed. The levulinic acid yields obtained in this research using a short reaction time of 5 min and low acid concentration of 2 wt.% H_2SO_4 were comparable to yields obtained from similar biomass and experimental conditions. Zheng et. al. investigated single stage production of levulinic acid from cornstalk in a batch reactor and observed a maximum levulinic acid yield of 48.89 mol.% at temperature 180°C, reaction time 40 min and 0.5 mol/L $FeCl_3$ as catalyst [81]. Girisuta et. al. carried out single stage acid catalysed hydrolysis of the water hyacinth to produce levulinic acid yield of 53 mol.% with 1 wt.% biomass loading, 9.5 wt.% H_2SO_4, reaction temperature of 175°C and reaction time of 30 min [82]. Levulinic acid yields in the range of 45.6 to 68.8 mol.% from various lignocellulosic biomass using H_2SO_4 concentration from 3.5 to 10 wt.% have been reported [44]. On the contrary to levulinic acid

yield, as shown in Fig. 3, solid residue production went down from 57% and 72.6% at 0 wt.% H_2SO_4 to minimum of 41.8% and 39.9% at 2 wt.% H_2SO_4 and rose again to maximum of 79% and 78.1% at 4 wt.% H_2SO_4 for raw and pretreated corn stover, respectively. These trends indicated that at lower H_2SO_4 concentration, there is incomplete hydrolysis of biomass, while at concentrations above the optimum, side reactions occur, resulting in higher solid residue. For both biomasses, levulinic acid yield was maximum when solid residue formation was minimum.

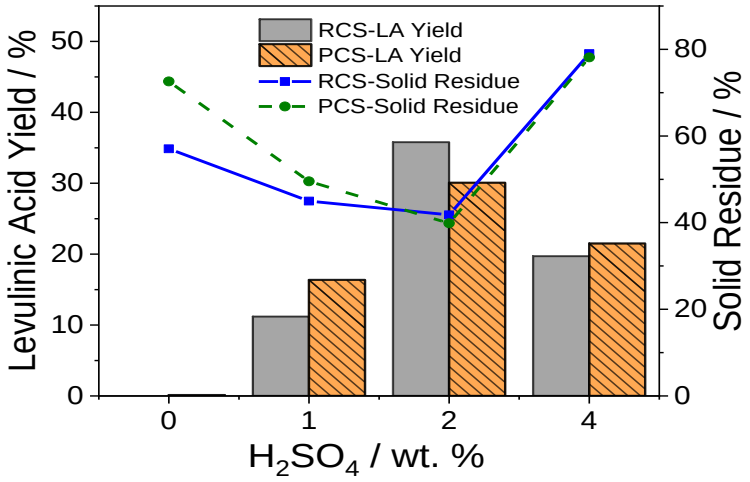

Figure 3. Levulinic acid yield (bar chart) and solid residue produced (line plot) using 0, 1, 2, and 4 wt.% H_2SO_4 and 5 min reaction time at 190 ℃ (RCS: Raw corn stover, PCS: Pretreated corn stover, and LA: Levulinic acid)

Fig. 4 shows the percentage of total dissolved organic carbon contributed by various organic compounds in hydrolysate produced through acid hydrolysis of raw and pretreated corn stover at reaction times varied from 5 min to 165 min, using optimum 2 wt.% H_2SO_4 at 190 ℃.

For a reaction time of 5 min, sources of 45% and 47% of organic carbon in the hydrolysate produced from raw and pretreated corn stover, respectively, were determined. The carbon in HMF contributed less than 1% of total organic carbon solubilized in hydrolysate at all conditions in both biomasses, indicating near complete rehydration of HMF to form levulinic acid and formic acid. Percentage of organic carbon contributed by levulinic acid was relatively higher in case of pretreated corn stover compared to raw corn stover, the highest contribution observed was 43% for reaction time of 105 min. Also, percentage of organic carbon contributed by lactic acid, acetic acid and furfural was significantly low in case of pretreated corn stover compared to raw corn stover. This was because the pretreated corn stover had only 9% hemicellulose compared to 24.1% in raw corn stover.

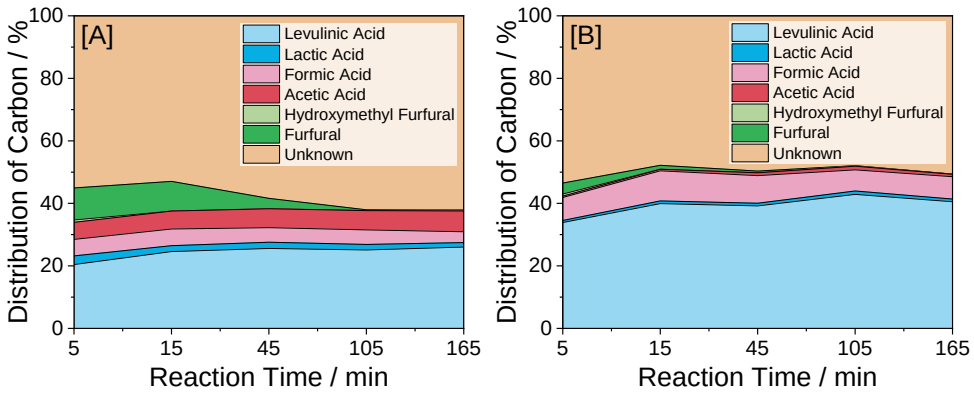

Figure 4. Source of organic carbon solubilized in hydrolysate produced through acid hydrolysis of raw [A] and pretreated [B] corn stover using 2 wt.% H_2SO_4 at 190 ℃

As shown in Fig. 2, hexose sugars in hemicellulose are converted to levulinic acid or other organic acids, while pentose sugars are converted to furfural. Furfural at harsh conditions polymerize with saccharides to form humins [52]. Thus, with increasing reaction time, the percentage of organic carbon contributed by levulinic acid increased for both biomasses. Shorter reaction time prevented transformation of furfurals without compromising on the levulinic acid yield. According to the stoichiometry, one hexose molecule forms one molecule of levulinic acid and formic acid each. Therefore, the contribution of carbon from levulinic acid and formic acid should be in a ratio of 5:1. However, at severe conditions formic acid degrades into carbon dioxide [83] and thus the contribution of formic acid towards total dissolved organic carbon decreased with an increase in reaction time in comparison to levulinic acid as seen in Fig. 4.

Fig. 5 shows levulinic acid yield based on glucan content in raw and pretreated corn stover through acid hydrolysis using 2 wt.% H_2SO_4. The reaction time had negligible impact on the levulinic acid yield for both raw and pretreated corn stover. Levulinic acid yield from raw corn stover was more than that in pretreated corn stover at all reaction times experimented. The reduced glucan to levulinic acid conversion in pretreated corn stover could be due to higher ash and lower hemicellulose concentration in it. The hydrogen ion concentration or reaction mixture acidity required for hydrolysis is a function of H_2SO_4 concentration and neutralizing power of ash [84]. Acetic acid is generated from the splitting of acetyl groups of hemicelluloses at elevated temperature. Thus, acetic acid formation in pretreated corn stover was less due to lower concentration of hemicellulose in it compared to raw corn stover. If acetic acid is allowed to react further, it undergoes autoionization and forms more hydronium ions which in turn act as catalyst and promotes the degradation of solubilized sugars [85,86].

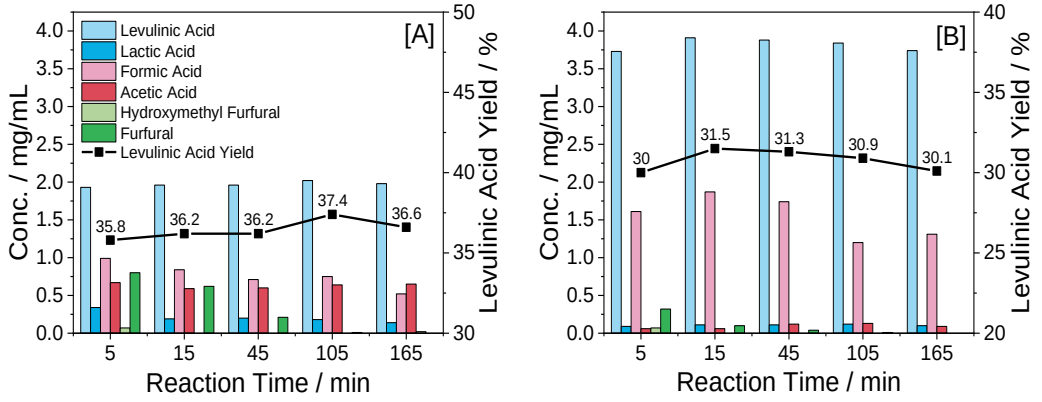

Figure 5. Concentrations of organic compounds analyzed (bar chart) and levulinic acid yield (line plot) in hydrolysate produced through acid hydrolysis of raw [A] and pretreated [B] corn stover using 2 wt.% H_2SO_4 at 190 °C

Kumar et al. [42] found that pretreating the biomass with K_2CO_3 at various concentrations, improved the accessibility of cellulose leading to better enzymatic digestion. The improved cellulose accessibility by removal of lignin and hemicellulose was not found to be beneficial in improving the levulinic acid yield or decreasing the optimum H_2SO_4 concentration. Some of the reports suggested that a possible way to improve levulinic acid yield is by improving cellulose accessibility through pre-treatment processes [44]. In this research work, improved cellulose accessibility was found to have a slight negative impact on levulinic acid yield. This is because, other parameters like biomass particle size, biomass composition, and processing conditions (reactor design and heating rate) could also influence the levulinic acid yield. The pretreatment by removal of lignin and hemicellulose increased the proportion of cellulose in biomass from 28.2% to 62.0%. Increased cellulose content in biomass can be advantageous in making the overall process more economical by allowing higher cellulose

loading. The acid hydrolysis process also forms various acid soluble lignin derived components [44]. The contribution of levulinic acid carbon to the total dissolved organic carbon was higher in pretreated corn stover compared to raw corn stover indicating that removal of lignin and hemicellulose can also help in reducing the complexity of the dissolved products. Also, compared to raw corn stover, higher cellulose content in pretreated corn stover led to an increase in the concentration of levulinic acid by 1.9 folds using 2% H_2SO_4 and reaction time of 5 min. Higher concentration of levulinic acid is beneficial in lowering downstream processing costs and thus direct acid hydrolysis of raw biomass should be avoided [87].

Table 3. Elemental composition analysis of raw corn stover, pretreated corn stover, and solid residue produced through acid hydrolysis using 2 wt.% H_2SO_4 and 5 min reaction time

Biomass	Nitrogen (%)	Carbon (%)	Hydrogen (%)
Raw corn stover	0.5	44.0	5.5
Solid residue from raw corn stover	0.4	42.9	3.9
Pretreated corn stover	0.2	39.5	5.1
Solid residue from pretreated corn stover	0.3	33.0	3.9

A reaction time of 5 min is plausible to be advantageous during process scale-up, as lower reaction times impacts equipment size and energy input. In the case where furfural is an additional compound of interest, lower reaction times can be used to prevent its polymerization

into humins. The solid residue produced using 2 wt.% H_2SO_4 and 5 min reaction time, raw corn stover, and pretreated corn stover were analyzed for elemental composition as shown in Table 3. No sulfur was detected in any of the samples analyzed. The solid residue produced from pretreated corn stover using 2 wt.% H_2SO_4 and 5 min reaction time was further used to synthesize biocarbon electrode material.

2.3.3 Analysis of Products from Enzymatic Hydrolysis of Biomass and Pilot Facility Design

The optimum pretreatment conditions vary with the type of lignocellulosic biomass. Many factors like genetics, cultivation techniques, environmental conditions etc. affect the structure and composition of biomass. Enzymatic hydrolysis followed by glucan digestibility calculations can be used to determine the effectiveness of these pretreatment conditions. The glucan digestibility of raw and pretreated corn stover was found to be 19% and 93%, respectively. About 37.1% of pretreated corn stover was unhydrolyzed. This lignin rich UHS shown in Fig. 6 was utilized by the collaborator for further experimentation.

Figure 6. UHS generated through enzymatic hydrolysis of pretreated corn stover

Fig. 7 shows a pathway that can be an alternative to the pathway shown in Fig. 2. The pilot facility design for processing one ton of corn stover per day was based on this pathway. P&ID for hydrothermal pretreatment and enzymatic hydrolysis of corn stover shown in Fig. 8 was generated in Microsoft Visio. These diagrams (PFD and P&ID) were merged with the diagrams generated by the collaborators working on the development of downstream processes. The collaborative project that this chapter is part of is titled, 'Pilot-Scale Biochemical and Hydrothermal Integrated Biorefinery (IBR) for Cost-Effective Production of Fuels and Value-Added Products'. The main project goal was to demonstrate cost effective production of value-added products like biocarbon, carbon nanofibers, polylactic acid, and phenols from the waste streams originated from biochemical and/or hydrothermal processing of a blend of corn stover and yard waste at pilot scale with simultaneous production of alcohols and diesel.

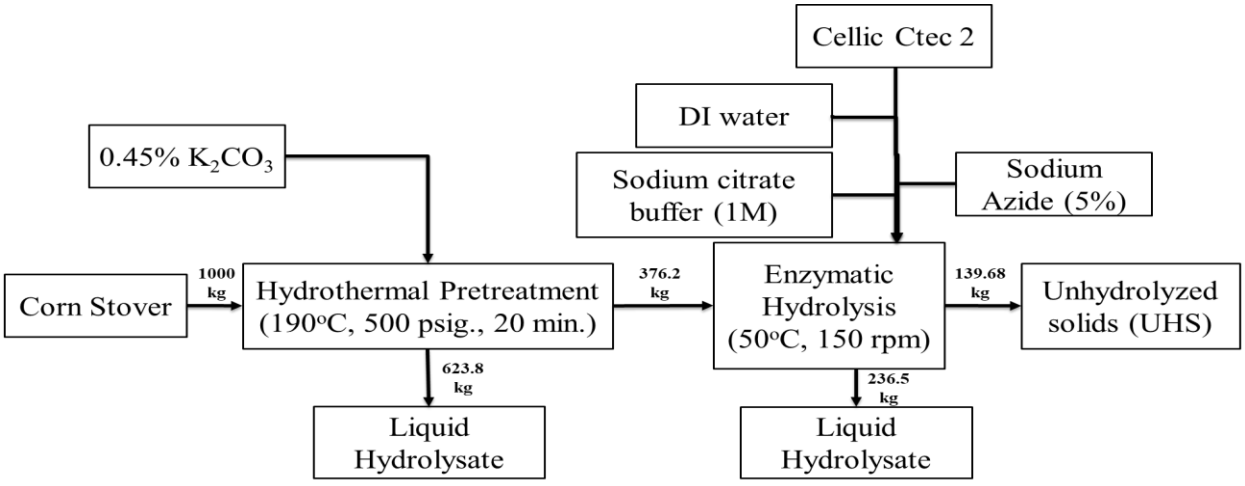

Figure 7. PFD with mass balance for hydrothermal pretreatment and enzymatic hydrolysis of corn stover

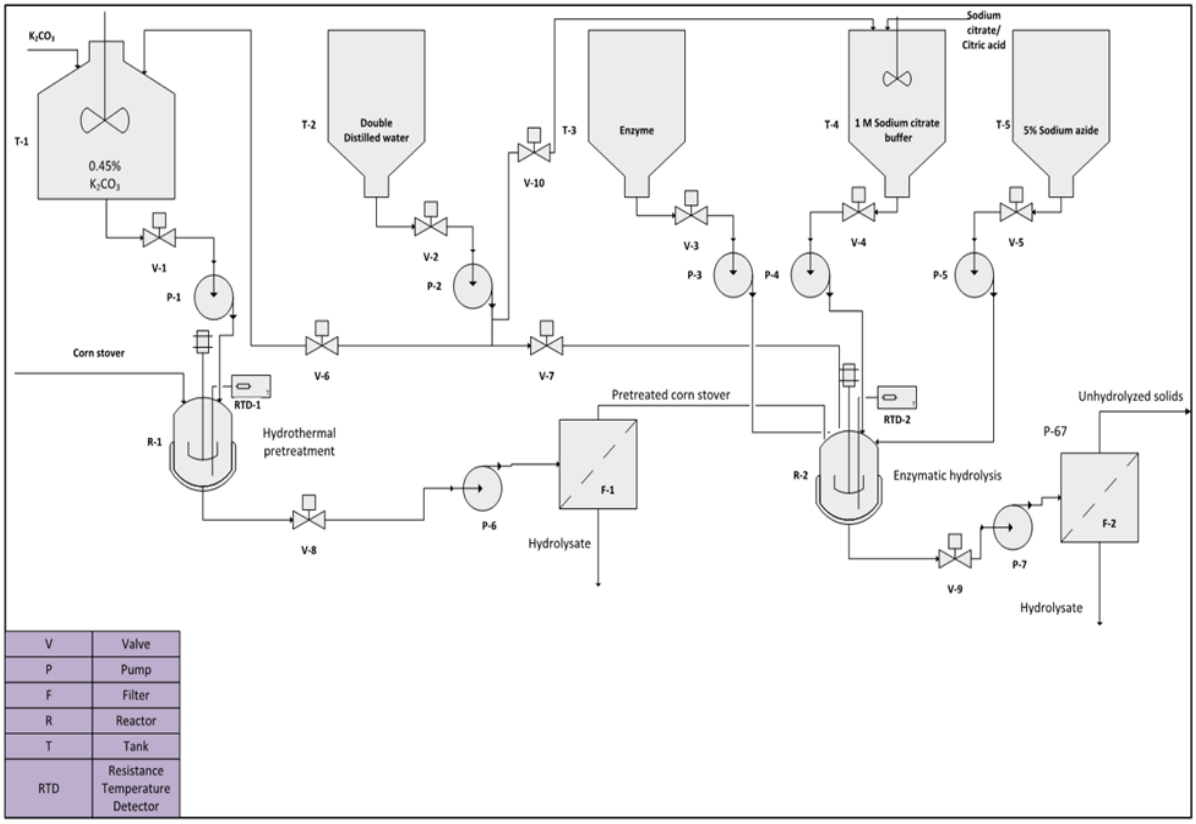

Figure 8. P&ID for hydrothermal pretreatment and enzymatic hydrolysis of corn stover

2.4 Conclusions

Overall, an integrated biorefinery process was successfully demonstrated, whereby raw corn stover was fractionated using 0.45 wt.% K_2CO_3 at 190 °C, extracting 76% of lignin and 85% of xylan while preserving 83% of glucan. During acid hydrolysis, 2 wt.% H_2SO_4 produced the highest levulinic acid yields while all other H_2SO_4 concentrations resulted in higher solid residue yields. A low-cost, sustainable two-step facile thermal annealing and activation process produced biocarbon with a specific capacitance of 120 F g^{-1}, S_{BET} of 466 m^2 g^{-1}, and pore volume of 0.24 cm^3 g^{-1} from acid hydrolysis solid residue. The pretreatment improved the enzymatic digestibility of glucan in corn stover from 19% to 93%.

2.5 Acknowledgments

This work was financially supported by the Department of Energy as part of award No. DE-EE0008252 (Pilot-Scale Biochemical and Hydrothermal Integrated Biorefinery (IBR) for Cost-Effective Production of Fuels and Value-Added Products).

CHAPTER 3

FLASH HYDROLYSIS OF YEAST (*SACCHAROMYCES CEREVISIAE*) FOR PROTEIN RECOVERY

Note: The contents of this chapter were adapted from the research article published in the journal of 'Supercritical Fluids'. The nutrient recycle experiments were conducted by the collaborators at the 'University of Padova'.

A. Thakkar, E. Barbera, E. Sforza, A. Bertucco, R. Davis, S. Kumar, Flash hydrolysis of yeast (Saccharomyces cerevisiae) for protein recovery, J. Supercrit. Fluids. 173 (2021) 105240.

Protein-rich spent yeast is a waste by-product of brewing and other fermentation industry. A continuous-flow hydrothermal treatment called 'flash hydrolysis' was deployed for protein recovery and yeast disposal. A feed slurry with 1-15 wt% yeast was hydrolyzed at temperatures ranging between 160-280 °C for a very short residence time of 10±2 s. Using 10 wt% yeast at 240 °C, 66.5% carbon, 70.4% nitrogen and 61.0% overall yeast biomass was solubilized in liquid hydrolysate. The liquid hydrolysate in which 63.1% of analyzed amino acids in yeast feed were solubilized, was tested as nutrient for cultivation of *E. coli* in a continuous bioreactor. The steady-state *E. coli* concentration was 1.18 g L^{-1} and 0.93 g L^{-1} using liquid hydrolysate and commercial yeast extract, respectively. Finally, the kinetic parameters for yeast solubilization (reaction order, activation energy and pre-exponential factor) were found to be 0.86, 21.3 kJ mol^{-1} and 19.36 $[L\ g^{-1}]^{n-1}\ s^{-1}$, respectively.

3.1 Introduction

Beer is one of the most popular beverages in the world. In 2019, its global production was 1.9 billion hL with annual market growth of about 1.4%. The brewing process produces three main by-products, namely spent grain, spent yeast and residual hops. Spent yeast is the second largest by-product of the brewing industry after spent grain and its yield is 1.7 to 2.3 g L^{-1} of beer produced [88]. During fermentation (brewing), yeast cells multiply many times

depending on the process conditions to produce significantly greater amount of yeast. The harvested yeast, also called spent yeast, is a tan colored, thick and viscous slurry with solid concentration of 3-15 wt% [88,89]. Although, it has some low-value application as animal feed, it is generally considered an organic waste. Its disposal is a concern as the techniques that are generally used such as incineration and landfills, have environmental impacts [90].

The soluble contents of yeast biomass obtained by disrupting and removing the yeast cell membrane is called yeast extract (YE) [91,92]. Only a fraction of the large quantities of spent yeast produced during beer manufacturing is reused as inoculum and thus the rest can be a cost-effective raw material for YE production [93,94]. The high protein content in yeast represents a good source of essential amino acids, which should be part of the diet as neither humans nor other mammals can synthesize them [95,96]. The amino acid composition of YE depends on the cell wall disruption method and following processes [92,95,97–99]. Amino acids in yeast have potential to serve as dietary supplement with health benefits. For example, the non-proteinogenic amino acid γ-aminobutyric acid (GABA) in yeast stimulates immune cells and can prevent diabetes [100]. Products like glutamic acid in the extract can be used as flavor enhancer [101] or the extract can be heat-processed further to form typical YE flavors [102]. YE can be widely used in the food industry, since the European Parliament regulation has classified it as a natural flavor [103], and it has also been assigned a “generally recognized as safe” (GRAS) status [98,104]. YEs are also added to the wort in the brewing industry as a nitrogen source to compensate for inadequate nitrogen supply to the yeast starter culture [105–107]. The quality and type of amino acids in YE play a role in development of flavor in the brew [108].

YE can be mainly produced using non-mechanical and mechanical processes. Various non-mechanical disruption methods like autolysis, plasmolysis [109,110] in organic salt solution

or non-polar organic solvent, acid or alkali catalyzed hydrolysis, or enzymatic hydrolysis [104,111] are applied to produce YE. Methods other than enzymatic autolysis generate wastewater with chemicals. Enzymatic autolysis is relatively environmental friendly but requires long process time and it is cost intensive at larger scale [90]. Commercially, autolytic or plasmolytic methods are primarily used [112] to achieve the highest possible extract yield [99]. Other than cell membrane lysis, another objective during autolysis can be the enzymatic hydrolysis of proteins into amino acids or the splitting of RNA to form flavor-enhancing 5′-nucleotides [91,112]. When thermally sensitive substances like enzymes or specific cell wall components like β-glucan are to be extracted, mechanical disruption methods such as cell mills are used [106,112,113].

Lamoolphak et al. [90] examined hydrothermal decomposition of baker's yeast into proteins and amino acids. For a batch reaction of 20 min in water at 250 °C, 78% of yeast was solubilized and protein produced was found to be 0.16 mg/mg dry yeast. Also, the hydrolysis products were tested as nutrient source for yeast cultivation and the growth rate was found to be comparable with commercial YE at same concentration. In a study using hog hair, subcritical water at 250 °C for 30 min was reported as a viable process for extraction of amino acids. Longer reaction time resulted in decomposition of hydrolyzed amino acids to ammonia [114]. Also, during hydrothermal reaction of biomass with longer residence time, the hydrolyzed carbohydrates and proteins react further to produce undesired compounds [115].

Hydrothermal treatment of yeast to produce proteins and amino acids can be developed further using flash hydrolysis (FH). In this context, we report a novel approach for protein extraction from yeast using a chemicals-free subcritical water based continuous-flow FH process. FH, where wet biomass slurry is subjected to high temperature for a very short residence time (8-

12 s) has been a proven technology for the fractionation of algae components like proteins and lipids [115]. Spent yeast slurry produced during brewing can be economically fractionated through a continuous FH process without any dilution or concentration. FH can not only be a solution for disposal of spent yeast but also provide a revenue stream by recovering valuable components. To the best of our knowledge, a scalable continuous-flow process characterized by short residence time (10±2 s) used in this study, has not been reported so far.

This study aims at optimizing the temperature and feed concentration for recovery of proteins from yeast through FH. To investigate the possible application of the YE obtained by FH as a medium for bacterial cultivation, the liquid hydrolysate obtained under the optimal experimental conditions was used as nutrient for *E. coli* cultivation, and the performances compared with those of a commercial product. Finally, the kinetics of yeast solubilization reaction were determined based on the experimental results.

3.2 Material and Methods

'Red Star Active' (Milwaukee, WI, USA) dry yeast was used as a model for brewer's spent yeast in FH experiments. The yeast was composed of lipids (6 wt%), carbohydrates (33 wt%) and proteins (50 wt%). Hydrochloric acid (HCl) and sodium hydroxide (NaOH) were purchased from Alfa Aesar (Ward Hill, MA, USA). Amino acid standard H, eluent chemicals for Ion Chromatography (IC) and standard for elemental composition (2,5-Bis(5-tert-butyl-benzoxazol-2-yl)thiophene) were purchased from Thermo Scientific (Waltham, MA, USA). Organic carbon (1000 ppm) and nitrogen (100 ppm) standards were procured from Ricca Chemical Company (Arlington, TX, USA). For *E. coli* growth experiments, the strain (ATCC 25922) was obtained from ATCC (Manassas, VA, USA), while commercial YE for media was

procured from Sigma Aldrich (St. Louis, MO, USA). De-ionized water was used for all the experiments unless otherwise specified.

3.2.1 Flash Hydrolysis

The schematic of the FH setup is shown in Fig. 9. The unit consists of pumping system, tubing, reactor, induction heating and control system, quenching zone and back pressure regulator (BPR). The induction heating and control system supplied by GH Induction Atmospheres (Rochester, NY, USA) could provide up to 5 kW of power. A LEWA (Holliston, MA, USA) EcoFlow diaphragm metering pump used in this study is capable of delivering concentrated yeast slurry at appropriate flow rates to maintain desired residence time in the reactor and generating appropriate pressures for subcritical water conditions. For ease of construction, the reactor and tubing were made of the same high-pressure tube supplied by High Pressure Equipment (Erie, Pennsylvania, USA). A tubular reactor with internal diameter of 0.31'' (7.9 mm) was selected to meet the required residence time. The 16'' (40.6 cm) long tube which was wound by the induction heater coil was considered as the reaction zone. An Omega (Norwalk, CT, USA) TJ36 thermocouple located at the end of the reaction zone was inserted inside the tubular reactor through a junction to measure the reaction temperature. The design pressure for the tubes and connectors was 137.9 MPa, which gave sufficient safety margin when operating at pressure of 10.3±0.15 MPa. The quenching zone was designed to utilize chilled water to lower the slurry temperature to below 100 °C, so the output hydrolysate would remain in liquid phase at collection point. A dome loaded BPR was used in the FH setup, manufactured specially for research by Equilibar (Fletcher, NC, USA).

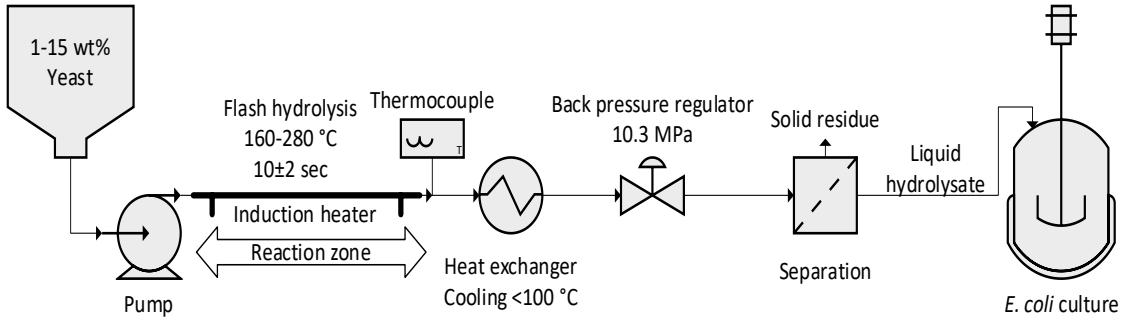

Figure 9. Schematic of the flash hydrolysis setup

Yeast slurry of 1, 5, 10, and 15 wt% was made using dry yeast and DI water. It was then pumped at a flow rate of 95 mL min^{-1} to maintain the residence time of 10±2 s in the reactor. The pressure of 10.3±0.3 MPa which was higher than the vapor pressure of water in the temperature range of study was maintained using BPR and then the induction heater was switched on. The desired temperature of 160, 200, 240 or 280 °C was maintained in the reactor using induction heater power control system. The deviation in reaction temperature was <10 °C during all the runs. After the system reached steady state in terms of flowrate, pressure and temperature, the hydrolysate was collected at the outlet of the reactor. The hydrolysate was made up of liquid fraction (liquid hydrolysate) and solid fraction (solid residue). At a given temperature and yeast feed concentration, the system was operated for 10 min. The residence time of the reactor was calculated using eq. 1, where V is the reactor volume (mL), F is the volumetric flow rate of pumps (mL min^{-1}), ρ_{pump} is the density of water at pump conditions (g mL^{-1}), and $\rho_{P,T}$ is the density of water at reactor conditions (i.e., pressure and temperature).

$$t = \frac{V}{F(\frac{\rho pump}{\rho_{P,T}})} \quad (1)$$

The solubilization of components (carbon, nitrogen and amino acids) in liquid hydrolysate was calculated using eq. 2 and solid residue was calculated using eq. 3.

$$Solubilization\ (\%) = \frac{Component\ in\ liquid\ hydrolysate\ (g/l)}{Component\ in\ feed\ (g/l)} \times 100 \quad (2)$$

$$Solid\ residue\ (\%) = \frac{Solids\ in\ hydrolysate\ (g/l)}{Solids\ in\ feed\ (g/l)} \times 100 \quad (3)$$

All FH experiments were performed in duplicate and the reported results are the average of two values.

3.2.2 Analyses of Flash Hydrolysis Products

After each experiment, a mixture of liquid and solid products was recovered and separated by vacuum filtration using mixed cellulose esters (MCE) membrane disc filters (0.22 μm). The solid fraction was washed using DI water and dried at 105 °C to determine percentage of yeast solubilized. The liquid hydrolysate was analyzed for total organic carbon (TOC) and total nitrogen (TN) composition using Shimadzu TOC/TN analyzer (Suzhou, China). The gaseous products, which were appreciably low in the temperature range of study, were vented without analysis. At select reaction conditions, solid residue composition was further analyzed using Flash 2000 Elemental Analyzer (EA) by Thermo Scientific (Bremen, Germany) and Cary 630 Fourier Transform Infrared Spectroscopy (FTIR) (Santa Clara, CA, USA). At these select reaction conditions, liquid fraction was also further analyzed for amino acid composition using IC (Dionex ICS-5000 AAA-Direct^{TM} equipped with an AminoPac PA10 column and column guard) supplied by Thermo Scientific (Waltham, MA, USA). A calibration curve was generated using an external amino acid standard for quantification. Free amino acids in the liquid hydrolysate were analyzed by directly running the samples through IC, whereas the peptides in

the liquid hydrolysate were acid hydrolyzed to free amino acids before IC analysis. The amino acid composition of yeast was also analyzed by acid hydrolyzing the biomass to free amino acids and then running the samples through IC. The acid hydrolysis of liquid hydrolysate and yeast was done using 6N HCl at 110 °C for 18 h, followed by neutralization using 6N NaOH before IC analysis. Other than histidine, all 16 amino acids in Amino Acid Standard H used for the IC analysis, could be accurately quantified. Therefore, histidine was only qualitatively analyzed.

3.2.3 Nutrients Recycle for *E. coli* Cultivation

The liquid hydrolysate produced at select FH condition was freeze-dried for preservation. This freeze-dried powder was called FH YE and was further tested as a nutrient (nitrogen) source for *E. coli* growth. Continuous experiments were carried out in chemostat mode to assess the YE exploitation at steady state. The strain was precultured overnight in standard lysogeny broth (LB) medium, containing 10 g L^{-1} of peptone and 5 g L^{-1} of commercial YE and 5 g L^{-1} of NaCl. Under sterile condition, about 5 mL of this culture was used as inoculum for cultivation tests. Cultivation tests were carried out in continuous reactors, comparable to a perfectly mixed continuous stirred-tank reactor (CSTR), with a working volume of 50 mL. The reactors were composed of sterilized glass bottles, where mixing was provided by magnetic stirring, coupled with filtered air bubbling, which also provided the required oxygen, at an average flow of 2 L h^{-1}. The temperature was maintained at 37 °C using a thermostatic bath. Fresh medium was continuously provided by means of a Sci-Q 400 peristaltic pump supplied by Watson Marlow (Falmouth, UK) at a constant volumetric flow rate of 28 mL h^{-1} from a sterilized, external, stirred glass bottle. An overflow tube was placed on the opposite side of the fresh medium inlet, ensuring the same outlet volumetric flow rate, thus keeping a constant culture volume. The resulting residence time, calculated as the ratio between the reactor volume and the flowrate, was

1.8 h. Optical density at 600 nm was measured every hour to observe the establishment of a steady state. After the steady state was reached, it was maintained for about 4 h, and at least 5 samples were taken during this time, to measure the biomass concentration in terms of dry weight (DW). DW was measured by filtering under vacuum 10 mL of previously harvested cells, with a 0.22 µm filter. The filter was then dried for 2 h at 100 °C in a laboratory oven.

Four different culture media were tested 1) standard LB, used as a control, with commercial YE; 2) LB with FH YE; 3) commercial YE only; and 4) FH YE only. The formulations are reported in Table 4. The amount of FH YE supplied, with respect to the commercial YE, was adjusted based on the nitrogen content (data certified by the manufacturer). Student's T test was performed in order to ascertain statistically significant differences among the tested conditions in terms of average biomass concentration reached at steady state. The level of statistical significance was taken at $p < 0.05$.

Table 4. Composition of media used in the *E. coli* cultivation tests

	Peptone ($g\ L^{-1}$)	**Commercial YE ($g\ L^{-1}$)**	**FH YE ($g\ L^{-1}$)**	**NaCl ($g\ L^{-1}$)**
LB (control)	10	5	--	10
LB FH	10	--	8.2	10
Commercial YE	--	10	--	10
FH YE	--	--	16.3	10

3.2.4 Yeast Solubilization Kinetics

The experimental results obtained at different temperatures (160-280 °C) and yeast feed concentrations (1-15 wt%) were used to retrieve the yeast solubilization kinetics in the FH process. The overall solubilization reaction, lumping all the water-soluble products into one since insoluble products were separated and gaseous products were vented, can be summarized as:

$$X \rightarrow Products \quad (4)$$

where *X* represents yeast. The rate of yeast solubilization (g L^{-1} s^{-1}) can be expressed as:

$$r_x = -k c_x^n \quad (5)$$

where *k* is the kinetic constant ([L g^{-1}]$^{n-1}$ s^{-1}), c_x the yeast concentration (g L^{-1}) and *n* is the order of reaction. The kinetic constant can be expressed as a function of temperature, according to the Arrhenius law (eq. 6).

$$k = A \cdot \exp\left(-\frac{E_a}{RT}\right) \quad (6)$$

with *A* being the pre-exponential factor, E_a the activation energy (kJ mol^{-1}), *R* the ideal gas constant (8.314 J mol^{-1} K^{-1}) and *T* the temperature in K. The reaction kinetic parameters (*A*, E_a, and *n*) were regressed based on experimental data, considering the material balance of a Plug-Flow reactor (PFR). According to the experimental set-up used, isothermal conditions and steady-state assumption were considered. The material balance can be written as:

$$\frac{dc_x}{dz} = \frac{1}{v} r_x = \frac{A \cdot \exp\left(-\frac{E_a}{RT}\right) c_x^n}{v} \quad (7)$$

where *z* is the length co-ordinate of the reactor (cm), and *v* is the velocity inside the tube (cm s^{-1}), calculated as the ratio between the volumetric flow rate and the reactor cross-sectional area. The material balance was solved from $z = 0$ ($c_x = c_{x,0}$) to $z = L$, using ode23 in MATLAB®. The

fminsearch function was used to minimize the sum of squared errors (SSE, eq. 8) between experimental and calculated values of the outlet biomass concentration, $c_{x,L}$.

$$SSE = \sum(c_{x,L,calc} - c_{x,L,exp})^2 \quad (8)$$

3.3 Results and Discussion

3.3.1 Flash Hydrolysis

As reported in Fig. 10, the impact of yeast concentration in the feed on solubilization of carbon and nitrogen was not substantial at all investigated temperatures. However, higher yeast concentration in feed resulted in a lower yeast solubilization at 240 and 280 °C. This could be due to differences in heat transfer (radial temperature gradient) within the slurry of different yeast concentration. By increasing the reaction temperature from 160 to 240 °C, solubilization of carbon and nitrogen steadily increased. The change in carbon and nitrogen solubilization with increase in reaction temperature from 240 to 280 °C was not as substantial as the change with increase in reaction temperature from 200 to 240 °C, suggesting the occurrence of saturation. Whereas the overall biomass solubilization steadily increased with increase in temperature from 160 to 280 °C, as shown in Fig. 10C. Operation of the FH system at 15 wt% yeast feed was challenging due to higher deviation in reaction temperature and frequent clogging of the BPR. Therefore, for higher accuracy, FH products obtained at different temperatures (160-280 °C) using 10 wt% yeast feed were further analyzed using IC, EA and FTIR. The overall biomass solubilization using 10 wt% yeast feed at 240 and 280 °C and residence time of 10±2 s was 61.0% and 78.3%, respectively. This was comparable to the value of 78% solubilization in a batch hydrothermal reaction carried out at 250 °C for a considerably higher reaction time of 20 min using the same yeast concentration, while it was significantly higher than the 32% obtained through autolysis after 19 h as reported by Lamoolphak et al. [90]. Compared to a batch

hydrothermal process, continuous-flow FH with a short residence time could possibly have lower capital and operating cost due to smaller equipment size and lower energy requirement, in terms of scale-up at industrial scale.

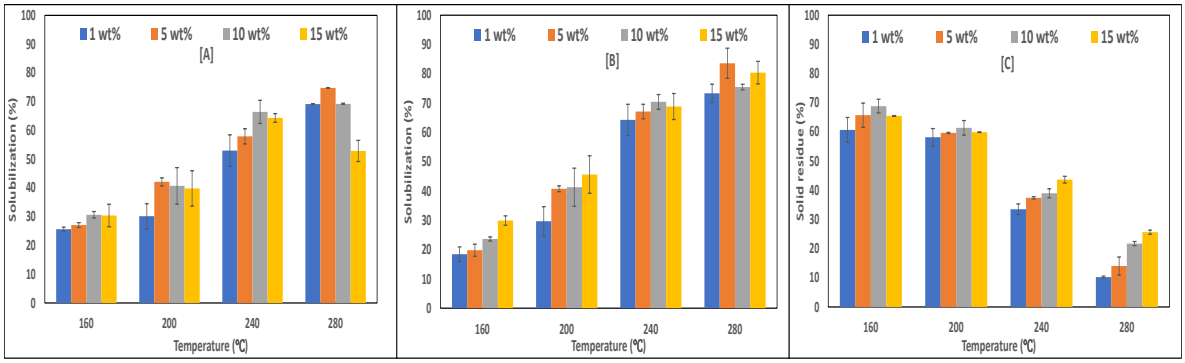

Figure 10. [A] Solubilization of carbon, [B] solubilization of nitrogen and [C] solid residue after FH of 1, 5, 10 and 15 wt% yeast feed at reaction temperature 160, 200, 240 and 280 °C

The nitrogen solubilization trend which is an indirect representation of protein solubilization shown in Fig. 10B indicated that increasing temperature of FH beyond 240 °C did not substantially improve nitrogen solubilization, which is also observed in amino acid profile of the acid hydrolyzed liquid hydrolysate shown in Fig. 11. The total average deviation in amino acid solubilization reported was less than 6% for duplicate experiments. Decrease in solubilization of some amino acids like alanine, threonine, lysine, serine, aspartate and cystine at 280 °C indicate partial degradation. Except for cystine, solubilization of all other amino acids

analyzed increased with increase in temperature from 160 to 240 °C. Solubilization of cystine was complete at 160 °C but it decreased with increase in temperature and reached the lowest 3.2% at 280 °C. Cystine could be completely solubilized at 160 °C as it accounted for only 0.5% of total amino acids analyzed in yeast. Also, due to its low concentration, a small degradation with rise in reaction temperature significantly affects its solubilization percentage compared to other amino acids. The transformation of amino acids under hydrothermal condition occurs through decarboxylation to produce carbonic acid and amines and deamination to produce ammonia and organic acids. The ratio and extent of deamination to decarboxylation differs depending on the type of amino acid and severity of experimental conditions. These undesired reactions which cause amino acid degradation can be significantly reduced by using FH compared to conventional batch hydrothermal reactions with longer residence time [115,116]. The IC analysis of liquid hydrolysate before acid hydrolysis showed presence of free amino acids in very low concentrations (<5% solubilization), arginine being the only exception. The solubilization of free arginine increased from 17.0% to 37.4% with increase in temperature from 160 to 280 °C. The total solubilization of all the amino acids analyzed in yeast at 160, 200, 240 and 280 °C was 21.4, 34.4, 63.1 and 60.3%, respectively.

Since the FTIR spectrum was similar for solid residues produced in duplicate experiments, only one set of spectra is reported as an example. As reported in Fig. 12, the lipid absorbance (C-H stretch) at wavelength 2920 and 2853 cm^{-1} intensifies with increase in temperature. With rising reaction temperature, the biomass solubilization increases, and thus biochemical components other than lipids are selectively solubilized, as observed by Garcia-Moscoso et al. [115] in case of algae FH. Absorbance linked to amide I (C=O stretch) and amide II (N-H and C-N vibrations) at 1637 cm^{-1} and 1526 cm^{-1} respectively, slightly rose with increase

in reaction temperature from 160 to 240 °C. The absorbance was maximum at 280 °C which suggests higher degree of protein-derived insoluble product formation at 280 °C. Under hydrothermal conditions (>250 °C), Maillard reactions occur between carbonyl group of carbohydrates and amine group of proteins or amino acids resulting in the formation of dark brown high-molecular-weight material called melanoidins [117,118]. This nitrogenous material with low solubility results in processing difficulties like fouling of process equipment, as observed in FH at 240 and 280 °C using 15 wt% yeast feed. The absorbance due to β-glucans at 1031 cm^{-1} and 990 cm^{-1} was found to be similar in yeast and solid residue produced at reaction temperatures other than 280 °C. The absorbances linked to glucans at 280 °C nearly disappeared, indicating higher degree of carbohydrate hydrolysis at 280 °C.

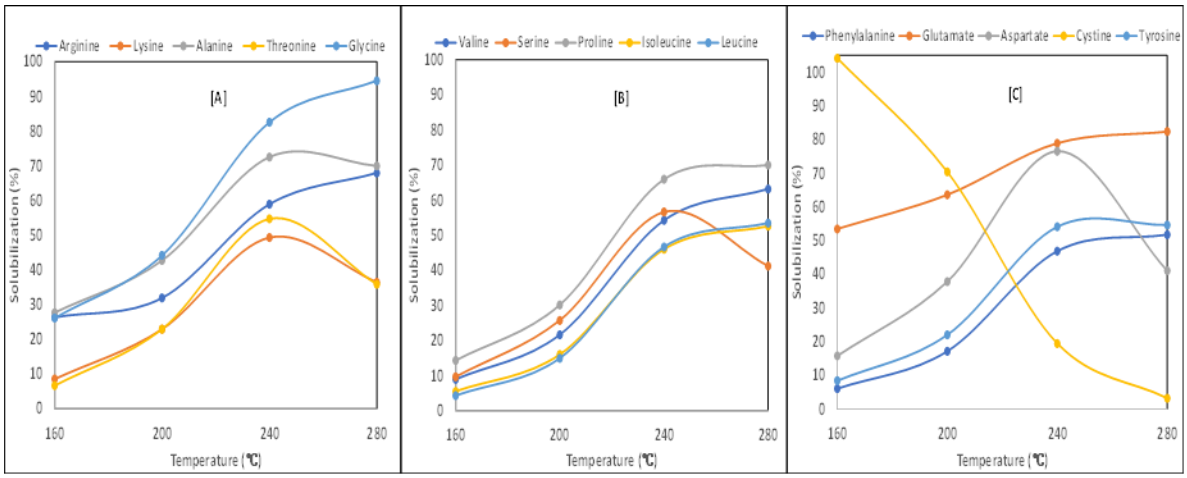

Figure 11. Amino acid solubilization in liquid hydrolysate generated using 10 wt% yeast feed and FH reaction temperature 160, 200, 240 and 280 °C, analyzed after acid hydrolysis (amino acids split between three plots [A], [B] and [C])

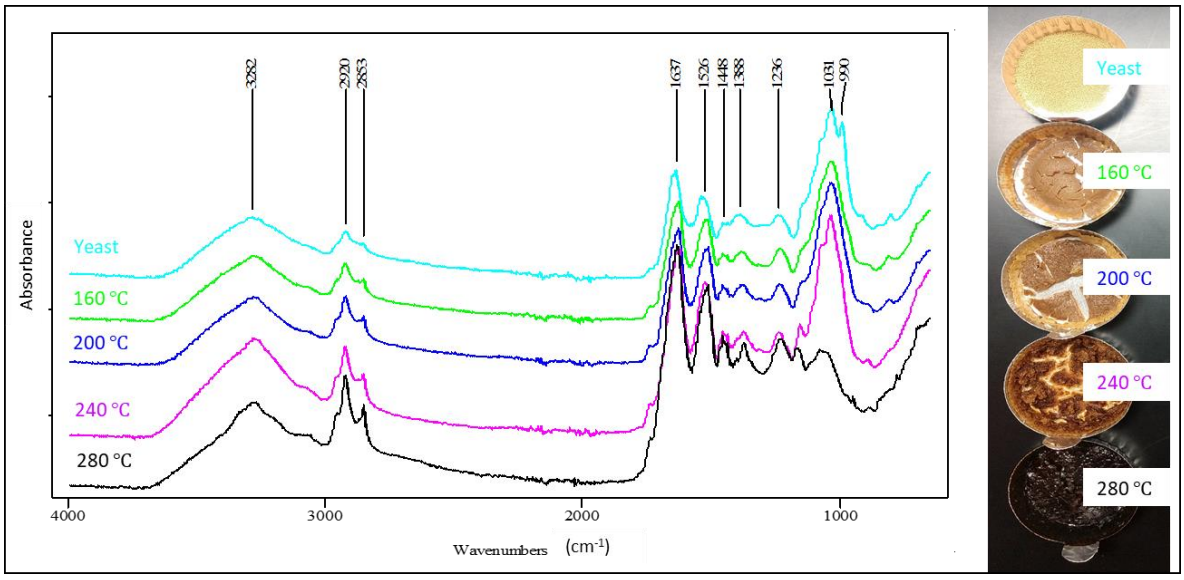

Figure 12. FTIR spectrum of solid residues produced using 10 wt% yeast feed and FH reaction temperature 160, 200, 240 and 280 °C

In Table 5, it is shown that the nitrogen content in the solid residue produced at 160 °C was higher compared to yeast, as only 23.7% nitrogen was solubilized when yeast solubilization was 31.2%. The C/N ratio in solid residue increased from 5.8 to 6.8 at 240 °C due to selectively higher solubilization of proteins in hydrolysate and accumulation of lipids and other non-protein compounds in solid residue, which was also observed in the FTIR spectrum. Further increase in temperature up to 280 °C, caused decrease in solid residue formation from 39.0% to 21.7%, whereas the increase in nitrogen solubilization was only 5%. This suggests a possible formation of insoluble proteinaceous/nitrogenous degraded material from solubilized protein and amino acids at 280 °C which was also revealed by the decrease in solubilization of some amino acids in the liquid hydrolysate and the increased absorbance due to amides in FTIR spectrum. The sharp

increase in solid residue carbon content at 280 °C, suggests the occurrence of carbonization reaction [90] and reduction in O/C ratio [68] due to higher reaction temperature.

Table 5. Elemental analysis of yeast and solid residues produced using 10 wt% yeast feed and FH reaction temperature 160, 200, 240 and 280 °C

	N (%)	**C (%)**	**H (%)**	**C/N**
Yeast	7.0±0.03	44.7±0.14	6.9±0.00	6.4
160 °C	8.4±0.02	48.8±0.24	7.4±0.14	5.8
200 °C	7.7±0.14	48.9±0.38	7.4±0.11	6.3
240 °C	7.5±0.03	50.8±0.07	7.5±0.03	6.8
280 °C	12.0±0.07	56.9±0.23	7.4±0.05	4.8

Overall, using 10 wt% yeast feed, FH at 280 °C helped lower solid residue formation but had slight negative effect on overall protein solubilization. Hence, FH of yeast at 240 °C was found to be the optimum temperature for protein solubilization, as it could also result in lower operating costs compared to 280 °C.

3.3.2 Nutrients Recycle for *E. coli* Cultivation

The FH YE used in the *E. coli* growth experiments was obtained at 240 °C and 10 wt% yeast feed. A comparison in terms of composition with the commercial product was made, revealing a

difference in macronutrient content. In particular, the commercial YE contains 11 wt% of nitrogen, as certified by the manufacturer for the specific lot used. The information about carbon content was not available, but literature reports an average content of about 40 wt% [119]. The composition of the FH YE showed a lower nitrogen content (6.7 wt%), but a slightly higher carbon content (47 wt%). With the aim of assessing the possible exploitation of FH YE as nitrogen source, the media were formulated normalizing the final nitrogen content, as reported in Table 4, also to account for the main aim of recycling protein and nitrogen thanks to FH. Continuous cultivation was chosen as culturing method, in order to allow cells to acclimate to the new medium composition. Results of average biomass concentration at steady state are reported in Fig. 13: remarkably, the biomass concentration obtained using the FH YE was significantly higher than that produced with the LB (control). This suggests not only that the flash hydrolysate can be used as alternative source of nitrogen, but it is also beneficial for growth, possibly due to the higher carbon content provided. To ascertain this hypothesis, a second set of experiments was carried out, without providing peptone (which itself is a nitrogen source) but doubling the concentration of YE to avoid possible nutrient limitations that may cause the culture washout in continuous reactors. The average biomass concentration reached was found not to be significantly different than that obtained in LB medium, confirming that carbon and nitrogen are indeed supplied in excess in the standard media composition. Also, in this case, an increased biomass concentration was observed when providing FH YE as sole source of nutrient compared to commercial YE. Thus, it appears that the liquid hydrolysate from FH is able not only to provide macronutrients, but possibly other micronutrients (vitamins) that result in an improved overall bacterial growth. Phenolic compounds were not analyzed in this study; however, it has been previously reported that the liquid hydrolysate generated through conventional

hydrothermal reactions with longer residence time than FH have higher concentration of phenolic compounds. This limits its application as nutrient media due to the inhibitory effect of phenolic compounds on microbial growth [115]. YE is commonly used as a source of micronutrients, co-factors, vitamins and minerals, but the exact composition is not always available, making comparison of the two products difficult. On the other hand, from an overall mass balance perspective, FH YE seems to be a promising alternative as cultivation media. As a drawback, it should be mentioned that the turbidity of the medium composed by FH YE was found to have increased, which is a critical point when applying optical density methods to assess growth.

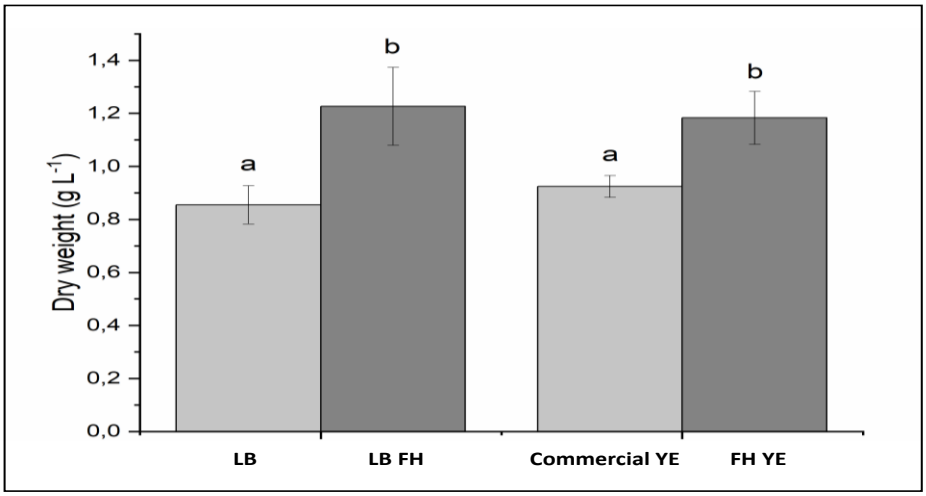

Figure 13. Average *E. coli* concentration using standard LB media with commercial YE (light grey) and FH YE (dark grey) compared to media containing only commercial YE (light grey) and FH YE (dark grey). Error bars refer to standard deviation and letters show statistically significant differences with $p < 0.05$

3.3.3 Yeast Solubilization Kinetics

The values of the kinetic parameters were obtained from the regression. The reaction was found to be of order 0.86, with an activation energy of 21.3 kJ mol^{-1} and pre-exponential factor of 19.36 $[L\ g^{-1}]^{n-1}\ s^{-1}$. The goodness of the fitting can be inferred from the plots of Fig. 14, where the result of the regressed model is represented together with experimental points in the whole range investigated (Fig. 14A), and calculated values are plotted against experimental ones, showing that points are well aligned along the bisector (Fig. 14B). In addition, standardized residuals are all comprised within the interval [-2, 2], except for one data point (160 °C and 15 wt% yeast feed), with most of them being between -1 and 1.

The kinetic parameters obtained could further be used for design of commercial scale FH setup. In particular, the kinetic model can be applied to assess the best operating conditions of a real scale plant in terms of optimum operating temperature: a tradeoff temperature can be selected, balancing energy required for heating and gain in reaction conversion. A further technoeconomic analysis will also assess the costs of the process proposed, related to best operating temperature. Additional information that can be obtained by the modeling approach are related to the best residence time, that has a role in the design of a full-scale reactor for yeast biomass hydrolysis.

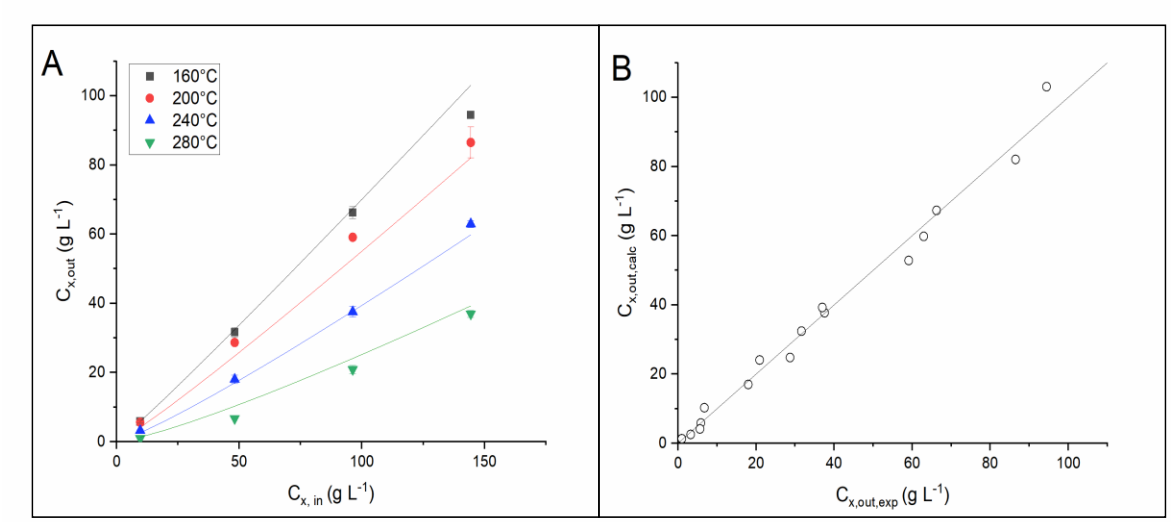

Figure 14. (A) Model (lines) and experimental results (dots) of outlet yeast (solid residue) concentration as a function of inlet feed concentration at different temperatures and (B) calculated (line) against experimental values (dots) of outlet yeast (solid residue) concentration

3.4 Conclusions

A continuous hydrothermal process for recovery of nutrients from yeast was developed whereby 66.5% carbon, 70.4% nitrogen and 61.0% overall yeast was solubilized at 240 °C. Flash hydrolysis with residence time of 10±2 s can serve as waste disposal and nutrient recovery technique for yeast slurry (1-15 wt%) without dilution or cost-intensive drying. The liquid hydrolysate from flash hydrolysis could be used as nutrient for cultivation of *E. coli* without growth inhibition. The kinetic parameters, reaction order (0.86), activation energy (21.3 kJ mol^{-1}) and pre-exponential factor (19.36 [L g^{-1}]$^{n-1}$ s^{-1}) could further be used for scale-up of flash hydrolysis setup.

3.5 Acknowledgements

This research work was financially supported by a grant from Sandia National Laboratories (SNL).

CHAPTER 4

COMPARATIVE STUDY OF FLASH AND ACID HYDROLYSIS OF MICRO-ALGAE FOR THE RECOVERY OF BIOCHEMICALS AND PRODUCTION OF POROUS BIOCARBON NANOSHEETS

Note: The contents of this chapter were adapted from the manuscript submitted to the journal 'Biomass Conversion and Biorefinery'.

A. Thakkar, P. Pienkos, N. Nagle, T. Dong, J. Kruger, S. Kumar, Comparative study of flash and acid hydrolysis of micro-algae for the recovery of biochemicals and production of porous biocarbon nanosheets, Biomass Convers. Biorefin. (under review).

8.5 wt.% micro-algae (*Scenedesmus sp.*) slurry was parallelly fractionated using two techniques, 'flash hydrolysis (FH)' and 'acid hydrolysis (AH)'. FH was performed at 240 °C with a residence time of 10±2 s in a continuous flow reactor, whereas AH was performed at 155 °C and reaction time of 15 min in a batch reactor. About 63% of micro-algal biomass was solubilized in liquid hydrolysate through both FH and AH. However, AH had an advantage over FH in recovering micro-algae proteins and carbohydrates. FAME recovery through solvent extraction from FH and AH derived wet solids (insoluble micro-algae) was 40 and 63%, respectively. Finally, the FH and AH derived post extraction solid residue was thermally activated using K_2CO_3 to produce highly microporous biocarbon nanosheets with BET surface area of 712 and 1289 $m^2\ g^{-1}$, respectively. Overall, an integrated process was developed using two potential hydrolysis techniques to maximize utilization of micro-algae components.

4.1 Introduction

The biorefineries and renewables are generating increasing interest worldwide, however, one of the major challenges it faces is utilization of biomass in its entirety. For development of an economically viable biorefinery, increasing the process energetic yields and value-added co-production with an integrated approach is crucial [120–123].

In general, hydrocarbon fuel is produced from micro-algae through two distinct pathways: hydrothermal liquefaction (HTL) and algal lipid upgrading (ALU). HTL can directly convert entire micro-algae biomass into a biocrude. However, HTL has many limitations including high nitrogen content in biocrude due to the presence of proteins in micro-algae [124], and also generates aqueous and solid byproducts for which valorization technology is currently underdeveloped. Alternatively, in the ALU pathway, lipids are first extracted from micro-algae followed by its upgradation [125]. Nevertheless, cost effective and efficient lipid extraction from micro-algae is one of the bottlenecks in this approach [126]. Moreover, the non-lipid fraction (proteins and carbohydrates) of micro-algae is degraded in both HTL and ALU process.

Further reduction in cost of algal biofuel by increasing the lipid content and overall biomass productivity, seems challenging. Improving cultivation and harvesting processes can help cut capital investment, but these advances alone might not be adequate to reduce the production costs to prices competitive with petroleum-based fuels. Recovering non-lipid micro-algae fraction and utilizing it efficiently for the production of value-added biochemicals could be the way forward for cost reduction and risk mitigation [121].

Early on, algal biofuel processes were focused on lipids while the carbohydrate and protein fractions were relegated to anaerobic digestion for biogas production. In later stages, along with lipid derived biofuels, the carbohydrate fraction of micro-algae was recovered using dilute acid pretreatment and then fermented to produce fuel or biochemicals [127,128]. This approach had an advantage over the processes that focus on lipid alone, but it limited the biomass feedstock options to low protein and moderate-to-high carbohydrate and lipid content. This placed more burdens on cultivation to both, reduce biomass costs by increasing productivity and improve biomass quality by moving away from high-protein micro-algae [120,121,129].

These factors highlight the requirement of processes that allow flexibility in accommodating micro-algae with high protein.

Two of the widely reported micro-algae fractionation technologies are flash hydrolysis (FH) and acid hydrolysis (AH). FH is a chemicals-free subcritical water based continuous-flow process. In FH, wet biomass slurry is subjected to high temperature (160–280 °C) for a very short residence time (8–12 s). On the other hand, AH is a dilute acid pretreatment process that is carried out at a relatively lower temperature (120–200 °C) for longer reaction time (10–15 min). In separate studies using various algae species and slurry concentrations, both FH and AH have been reported as efficient fractionation techniques that produce liquid hydrolysate and lipid-rich solids [115,116,120,121,130].

Liquid hydrolysate made up of solubilized biomass components has proved to be an excellent nutrient media for fermentation without addition of yeast extract and peptone as supplements. In Chapter 3, it was demonstrated that liquid hydrolysate rich in solubilized proteins can be effectively used as a fermentation media for cultivation of *E. coli* without growth inhibition [130]. Also, with AH of micro-algae, Dong et al. [121] observed that liquid hydrolysate supported rapid and robust fermentation of *S. cerevisiae* to produce ethanol. It has been also reported that the lipids are retained in the solid fraction of FH and AH hydrolysate [121,124]. After the extraction of lipids from the solids using solvents, a considerable amount of the so-called post-extraction solid residue (PESR) is available for valorization as a co-product.

In an integrated process that maximizes micro-algae utilization, the effective use of PESR would be critical to make the process more economical [131,132]. PESR which is mainly composed of carbohydrates and proteins as well as unextracted lipids could be an attractive precursor for producing porous biocarbon doped with heteroatoms. Heteroatoms in the carbon

lattice are known to significantly enhance mechanical, semi-conducting, field-emission, and electrical properties of carbon materials [133]. Specifically, nitrogen doping is considered to be the most promising method for enhancing surface polarity, electric conductivity, and electron-donor tendency of the activated carbon (AC) [134]. Activation of PESR to produce porous carbon material has been previously reported by Chang et al. [132] but the precursor was not fractioned before activation to recover valuable proteins and carbohydrates.

Various agents like KOH, NaOH, and $ZnCl_2$ are used for activating biomaterials. Even if these activating agents are efficient in producing carbon with desirable properties, their harmful effects (corrosiveness and environmental concerns) make them less desirable. For these reasons, K_2CO_3 is being increasingly considered for its application as an activating agent [129,135].

This study for the first time aims to compare FH and AH process for fractionation of high-protein low-lipid micro-algae. The comparison was based on recovery and solubilization of carbohydrates and proteins as well as the accessibility of lipids in wet solids for solvent extraction. To the best of our knowledge, a continuous flow FH of concentrated (8.5 wt.%) micro-algae slurry has not been reported so far. Also, for efficient utilization of hydrolyzed fractions, the PESR derived from FH and AH was processed thermally to produce porous biocarbon using K_2CO_3 as an agent in a single step activation process. The objective of this study was to develop processes to maximize the utilization of micro-algae components efficiently.

4.2 Material and Methods

Micro-algae *Scenedesmus sp*. supplied by National Renewable Energy Laboratory (CO, USA) was used for the experiments. Hydrochloric acid (HCl), sulfuric acid (H_2SO_4) and sodium hydroxide (NaOH) were purchased from Alfa Aesar (MA, USA). Amino acid standard H, eluent chemicals for Ion Chromatography (IC), standard for elemental composition (2,5-Bis(5-tert-

butyl-benzoxazol-2-yl)thiophene), and anhydrous potassium carbonate (K_2CO_3) were purchased from Thermo Scientific (MA, USA). Carbon (1000 ppm) and nitrogen (100 ppm) standards were procured from Ricca Chemical Company (TX, USA). De-ionized (DI) water was used for all the experiments unless otherwise specified.

4.2.1 Flash and Acid Hydrolysis

8.5 wt.% micro-algae slurry was used as feed for both FH and AH experiments, the resultant hydrolysates were made up of liquid fraction (liquid hydrolysate) and solid fraction (solids). The schematic of the FH setup, component details, and operation parameters have been described in Chapter 3. Briefly, the FH unit consists of a pumping system, tubing, reactor, induction heating and control system, quenching zone, and back pressure regulator (BPR). The micro-algae slurry was pumped at a flow rate of 95 mL min^{-1} to maintain the residence time of 10±2 s in the reactor. The pressure of 10.3±0.3 MPa which was higher than the vapor pressure of water at the reaction temperature of 240 °C was maintained using the BPR and then the induction heater was switched on. The deviation in reaction temperature was <10 °C during all the runs. For each run, the system was operated for 10 min to collect about 1 L of product. The residence time of the reactor was calculated using Eq. 1, where V is the reactor volume (mL), F is the volumetric flow rate of pumps (mL min^{-1}), ρ_{pump} is the density of water at pump conditions (g mL^{-1}), and $\rho_{P,T}$ is the density of water at reactor conditions (i.e., pressure and temperature).

$$t = \frac{V}{F(\frac{\rho_{pump}}{\rho_{P,T}})} \quad (1)$$

Acid hydrolysis of the micro-algae was performed in continuously stirred (300 rpm) batch mode using a 0.5 L Parr reactor. The furnace was preheated for 30 min to reduce the

temperature ramp time. Appropriate volume of 72% H_2SO_4 was added to the micro-algae slurry to make a reaction mixture containing 0.85 wt.% H_2SO_4 and 8.5 wt.% micro-algae. The H_2SO_4 concentration was 10% of micro-algae concentration which was found to be optimum by Knoshaug et al. [136]. Each batch was made up of 400 mL of reaction mixture. The contents within the Parr reactor typically reached the desired reaction temperature of 155±2 °C in 10–11 min of placing the reactor in the furnace as measured by the thermocouple at the center of the reactor. Reaction temperature of 155±2 °C and autogenous pressure was maintained for 15 min before cooling it down to <50 °C in 10 min by submerging the reactor in water bath. At the end of experiment, the residual pressure in the reactor was slowly released and the reaction mixture was collected.

The solubilization of components (carbon, nitrogen, proteins, and carbohydrates) in liquid hydrolysate was calculated using Eq. 2 and micro-algae solubilization was calculated using Eq. 3.

$$Component\ solubilization\ (\%) = \frac{Component\ in\ liquid\ hydrolysate\ (g/l)}{Component\ in\ feed\ (g/l)} \times 100$$

(2)

$$Micro-algae\ solubilization\ (\%) = \frac{Solids\ in\ feed\ (g/l) - Solids\ in\ hydrolysate\ (g/l)}{Solids\ in\ feed\ (g/l)} \times 100$$

(3)

All FH and AH experiments were performed in triplicate and the reported results are the average of three values. Fig. 15 depicts the proposed fractionation scheme for micro-algae.

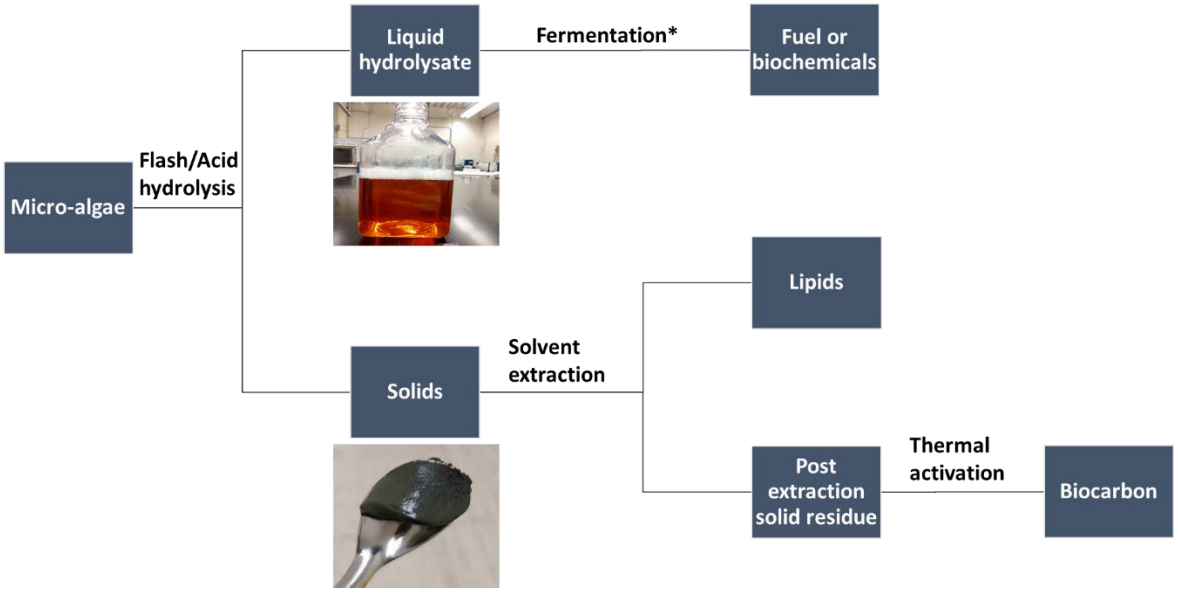

Figure 15. Proposed fractionation scheme for micro-algae (* not included in this study)

4.2.2 Analysis of Flash and Acid Hydrolysis Products

After each experiment for analytical purpose, a mixture of liquid and solid products was recovered and separated by vacuum filtration using mixed cellulose esters (MCE) membrane disc filters (0.22 μm). The solid fraction was washed using DI water and dried at 105 °C to determine percentage of micro-algae solubilization. The liquid hydrolysate was analyzed for total carbon (TC) and total nitrogen (TN) composition using a Shimadzu TC/TN analyzer (Suzhou, China). The gaseous products, which were low in the temperature range of study, were vented without analysis. The elemental composition of micro-algae and other solids generated in this research work was analyzed using Flash 2000 Elemental Analyzer (EA) by Thermo Scientific (Bremen, Germany). The liquid hydrolysate was also further analyzed for solubilized proteins and carbohydrates. Both free amino acid and peptide composition in liquid hydrolysate and micro-

algae was determined using IC (Dionex ICS-5000 AAA-Direct^{TM} equipped with an AminoPac PA10 column and column guard) supplied by Thermo Scientific (MA, USA) using methodology reported in Chapter 3. Similarly, free carbohydrate monomer and oligomer composition was determined using high pressure liquid chromatography (HPLC) with Bio-Rad Aminex HPX-87P column. Carbohydrate composition in liquid hydrolysate and micro-algae was analyzed as per NREL/TP-510-42623 [137] and NREL/TP-5100-60957 [138] standard procedure, respectively.

4.2.3 Lipid Extraction and Product Analysis

The solids generated through AH and FH were concentrated to 10-12 wt.% using centrifuge and then the lipids were solvent extracted from wet solids. Solids (10-12 wt.%): Hexane: Ethanol:: 3: 3: 1 (volume basis) was used for three sequential extractions followed by phase separation, based on the process published by Wendt et al. [139] where petroleum ether was used instead of hexane. The solvent was recovered overnight using a rotary evaporator at 55 ºC and the lipid extraction was quantified gravimetrically. The PESR from FH and AH was washed using DI water and then dried at 105 ºC. The extracted lipids and the lipids in the micro-algae feed were analyzed as fatty acid methyl ester (FAME) using method described in NREL/TP-5100-60958 [140]. Functional groups and surface morphology of PESR was analyzed using Cary 630 Fourier Transform Infrared Spectroscopy (FTIR) and Thermo Scientific Phenom Pure Desktop Scanning Electron Microscope (SEM), respectively.

4.2.4 Carbonization of Post Extraction Solid Residue and Product Analysis

0.2 g of PESR derived from FH and AH was impregnated with a desired volume of 50 wt.% K_2CO_3 solution for 3 h followed by overnight drying at 105 °C. 0 (no K_2CO_3), 0.25, and 0.5 K_2CO_3 impregnation ratios (IR) were used, calculated using Eq. 4. The resultant dry mixture was filled in an alumina holder which was suspended at the center of the thermogravimetric

analyzer (Model No.: TGA-50; Shimadzu Co., Japan) using platinum support. The temperature was ramped up at a rate of 5 °C min^{-1} from room temperature to 850 °C and held for 3 h before cooling it down back to room temperature. The resultant biocarbon was washed twice with 40 mL hot DI water to remove residual K_2CO_3 and other pore blocking contaminants. After washing, the product was dried overnight at 105 °C and weighed. The product yield was calculated using Eq. 5.

$$Impregnation\ ratio\ (IR) = \frac{Potassium\ carbonate\ \ (g)}{FH\ or\ AH\ PESR\ (g)}$$

(4)

$$Yield\ (\%) = \frac{Dry\ washed\ product\ (g)}{FH\ or\ AH\ PESR\ (g)} \times 100$$

(5)

The characteristics of these biocarbon were analyzed further. The Brunauer–Emmett–Teller (BET) surface area and total pore volume were analyzed via N_2 adsorption/desorption in a Quantichrome NOVA 2000e analyzer. Quenched Solid Density Functional Theory (QSDFT) was used for calculating pore size distribution. All products were degassed at 200 °C for 15 h prior to analysis. A High-Resolution Transmission Electron Microscope (TEM) (Model: JEM-2100F) with accelerating voltage 200 kV and probe size under 0.5 nm was used to analyze biocarbon with maximum BET surface area derived from FH and AH PESR.

4.3 Results and Discussion

4.3.1 Flash and Acid Hydrolysis Product Analysis

The micro-algae was made up of 54.3% proteins, 15.2% carbohydrate, 8.0% FAME, and 10.8% ash. The elemental and ash composition of micro-algae is shown in Table 6. Although, the reaction conditions for FH and AH were very different, the solubilization of carbon, nitrogen,

and the overall biomass after FH and AH was found to be similar. 44.4±0.9% carbon, 61.1±1.5% nitrogen, and 63.1±1.7% biomass was solubilized after FH whereas 48.0±2.4 % carbon, 61.6±3.3 % nitrogen, and 63.1±1.4 % biomass was solubilized after AH. The pH of FH and AH hydrolysates was 6 and 2.7, respectively.

Table 6. Elemental and ash analysis of micro-algae, PESR, and biocarbon on moisture free basis

	N (%)	**C (%)**	**H (%)**	**Ash (%)**
Micro-algae	9.8±0.04	49.6±0.90	7.1±0.09	10.8±0.40
FH PESR	9.6±0.47	57.8±0.09	7.6±0.01	5.7±0.50
IR		**FH Biocarbon**		
0	4.6±0.16	65.7±2.44	0.5±0.07	22.2±2.15
0.25	1.1±0.01	62.2±0.68	1.2±0.21	22.7±0.75
0.50	0.6±0.09	62.8±0.86	1.0±0.07	22.7±0.25
AH PESR	8.8±0.48	57.3±0.25	7.7±0.05	2.5±0.70
IR		**AH Biocarbon**		
0	4.1±0.18	66.9±0.08	0.8±0.29	15.9±0.90
0.25	0.8±0.01	68.5±0.79	1.0±0.16	21.6±2.55
0.50	0.6±0.02	66.3±0.49	0.8±0.18	19.2±0.55

It has been reported that estimating proteins using nitrogen-to-protein factor could be inaccurate in case of micro-algae since there can be significant amount of non-protein nitrogen from sources like nucleic acids, chlorophyll, and nitrogen-containing lipids, metabolites, inorganic nitrogen species [141] as well as degraded nitrogenous products if any [115]. Even though the nitrogen solubilization in FH and AH liquid hydrolysate was similar, as seen in Table 7, the amino acid and peptide composition of hydrolysates was different. Overall, it is seen that AH solubilized proteins better than FH. Also, the proportion of amino acid (monomer) in total amino acid and peptide mixture was higher in AH liquid hydrolysate compared to FH liquid hydrolysate, except for arginine and aspartate. It has been previously reported and also observed here that arginine is the most solubilized amino acid monomer when micro-algae is flash hydrolyzed [115]. The protein composition of micro-algae is also shown in Table 7.

Table 7. Protein composition of micro-algae, FH liquid hydrolysate, and AH liquid hydrolysate

		FH Solubilization (%)		**AH Solubilization (%)**	
	Micro-algae composition (%)	Amino acid	Amino acid and peptides	Amino acid	Amino acid and peptides
Arginine	6.7	70.2	100.0	53.1	86.8
Glutamate	5.7	12.8	97.7	51.3	97.6
Alanine	5.3	37.3	75.6	51.9	91.4
Lysine	4.9	13.2	37.0	31.4	65.8
Leucine	4.8	22.0	47.1	38.3	65.3
Aspartate	4.6	5.1	39.6	5.7	95.8
Valine	4.3	23.3	52.5	36.2	64.5

Phenylalanine	3.5	18.4	43.2	31.0	59.2
Proline	3.4	31.6	57.4	48.3	79.6
Glycine	3.0	28.6	74.2	31.0	73.3
Threonine	2.5	19.1	42.0	52.8	71.7
Isoleucine	2.4	22.7	46.7	35.5	64.6
Serine	1.6	17.2	41.9	23.1	52.3
Tyrosine	1.4	7.9	62.6	16.4	66.1
Cystine	0.3	0.0	0.0	0.0	0.0
Methionine	0.0	0.0	0.0	0.0	0.0
Histidine	Present, not quantified				

The carbohydrate fraction of micro-algae was made up of 7.5% glucose, 3.2% galactose, and 4.4% mannose. The solubilization of these components in the liquid hydrolysates are shown in Table 8. Solubilization of glucose was low compared to galactose and mannose in both FH and AH liquid hydrolysate. Most of the solubilized carbohydrates were in oligomeric form, which means an additional hydrolysis step might be required to produce monomers for fermentation. Similar to protein solubilization, carbohydrates were also solubilized better through AH compared to FH at conditions experimented in this study.

Table 8. Carbohydrate composition of FH liquid hydrolysate and AH liquid hydrolysate

	Solubilization (%)		
	Glucose	Galactose	Mannose
	Carbohydrate monomers		
FH	0.0	0.0	10.2
AH	2.0	32.7	19.1
	Carbohydrate monomers and oligomers		
FH	5.1	54.2	78.7
AH	6.8	96.3	100.0

4.3.2 Lipid Extraction and Product Analysis

The solvent extracts (lipids) obtained gravimetrically from FH and AH solids were 13.2 and 9.8% of biomass feed, respectively. However, only 24.5% of FH and 51.3% of AH lipids were accounted as FAME. This indicated that a significant amount of components other than fatty acids and free fatty acids were extracted in the solvent. FAME composition of micro-algae, lipids extracted from FH solids, and lipids extracted from AH solids is shown in Table 9. The three major FAME in micro-algae were C16:0, C18:3n3, and C16:4. Polyunsaturated Fatty Acid (PUFA), C18:3n3 and C16:4 contributed >50% of total FAME in micro-algae. The overall FAME recovery from micro-algae after FH and AH was 40.3 and 60.0%, respectively. This difference was mainly due to inefficient recovery of PUFA from FH solids. The recovery of Saturated Fatty Acid (SFA) and Monounsaturated Fatty Acid (MUFA) from FH solids was slightly higher than AH solids.

Several hypotheses have been used to explain the low level of extractable lipids after AH, including physical entrapment of lipids in residual biomass, side reactions causing interaction of lipids to cell wall residue, and adherence of lipids to the reactor surface [120,121]. Particularly,

in case of early harvest micro-algae that has high protein and low lipid content like the one used in this study, lipid extractability with hexane after acid pretreatment was found to be on the lower side. A combination of factors, including the complex and heterogeneous nature of the lipid fraction and inadequate hexane migration through polar biomass constituents, were reported to be responsible [142]. Harsher hydrolysis conditions of higher temperature, longer reaction time, and higher acid concentration in AH and strategies like multi-pass and chemical-aided FH could be used to further improve the FAME recovery.

Extraction of lipids from dry biomass is usually more efficient compared to wet biomass. Drying of biomass is an energy intensive process and thus not ideal for a large-scale process [132]. However, it should be noted that other than FAME, the solvent extract may also have components like ash, carbohydrates, proteins (amino acids), sterols, nucleic acids, pigments, and some other unknowns [141]. This makes the concentration of solids very important in wet extraction. Higher concentration of solids may reduce co-extraction of components other than lipids present in liquid hydrolysate. As observation but not elaborated in this article was the density difference between FH and AH derived solids. Preliminary studies revealed that FH solids could be concentrated up to 35.6 wt.% compared to 13.2 wt.% AH solids using same centrifugal force and time. This indicated that AH solids may have lower density than FH solids.

Table 9. FAME analysis of micro-algae, lipids extracted from FH solids, and lipids extracted from AH solids

	Micro-algae (% of the total FAME)	FH Recovery (%)	AH Recovery (%)
Saturated Fatty Acid (SFA)			
C16:0	18.0	62.8	47.4
C10:0	0.7	14.9	2.3
Monounsaturated Fatty Acid (MUFA)			
C18:1n9	3.9	82.7	76.6
C18:1n7	2.2	86.3	83.9
C16:1n11	2.0	56.2	63.0
C16:1n7	0.8	86.5	76.0
Polyunsaturated Fatty Acid (PUFA)			
C18:3n3	36.7	25.2	66.2
C16:4	17.0	14.4	58.8
C18:2n6	4.8	43.9	69.8
C16:3	3.7	43.7	69.1
C18:4n3	1.5	15.3	61.5
C16:2	1.4	41.2	66.4
C20:4n6	0.7	98.5	100.0
Unknown			
C16	3.5	78.6	83.7

The FTIR spectrum of FH and AH PESR revealed their biochemical similarity. As reported in Fig. 16, the C-H stretch at wavelength 2919 and 2851 cm^{-1} represents residual lipids. Absorbance linked to amide I (C═O stretch) and amide II (N−H and C−N vibrations) at 1623 cm^{-1} and 1517 cm^{-1}, respectively, suggests presence of proteins. The absorbance due to β-glucans at 1031 cm^{-1} confirms that glucose solubilization through FH and AH was low. However, substantial differences in the morphology of FH and AH PESR was seen in the SEM

images. The AH PESR was found to have highly perforated structure while FH PESR was a compact structure. This supported the claim of density difference in FH and AH PESR.

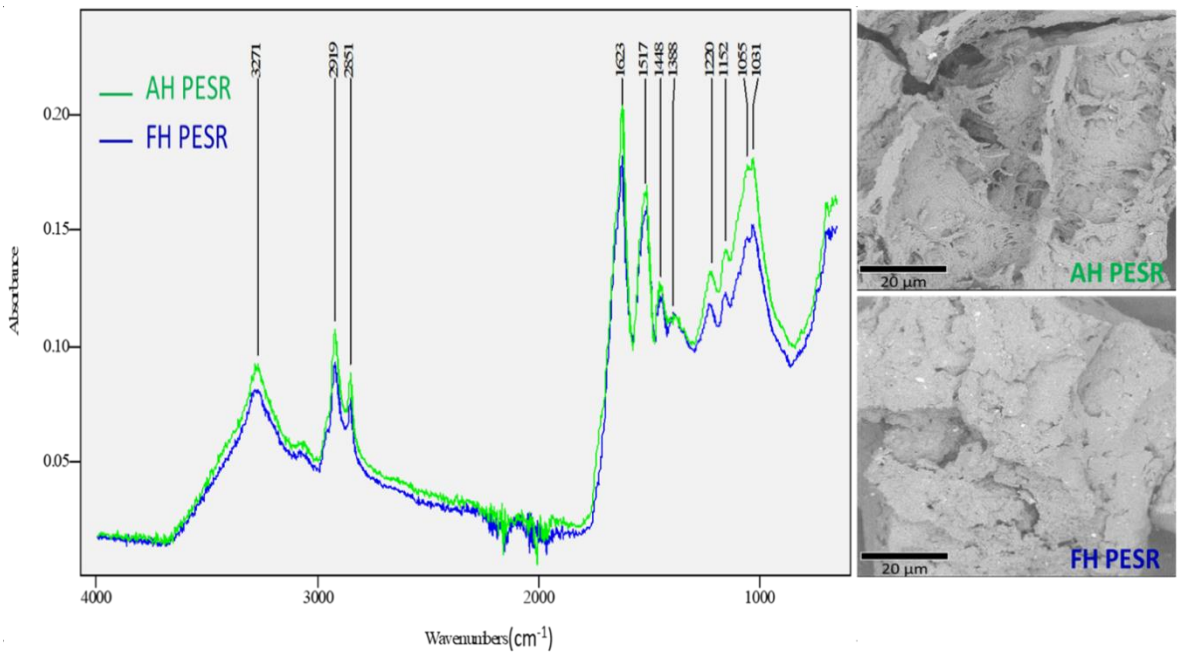

Figure 16. FTIR spectrum and SEM images of FH and AH PESR

4.3.3 Carbonization of Post Extraction Solid Residue and Product Analysis

After extraction, the PESR from FH and AH were carbonized at 850 °C, washed, and characterized. PESR carbonized without K_2CO_3 showed minimal surface area and no porosity, indicating the need for a carbonization catalyst. N_2 adsorption/desorption isotherms of biocarbon produced from FH and AH PESR with K_2CO_3 (IR=0.25 and 0.5) are shown in Fig. 17. All

isotherms (A1, A2, B1, and B2) exhibit a type IV profile. Also, the hysteresis loops seen here can be classified as H4 loop based on the IUPAC classification of adsorption isotherms. The more pronounced uptake at low relative pressure (P/P_0) in case of B1 and B2 compared to A1 and A2 indicate higher micropores in AH derived biocarbon. This was also evident in the pore size distribution (Fig. 18). H4 loops are often found with aggregated crystals of zeolites, some mesoporous zeolites, and micro-mesoporous carbons that have narrow slit pores. One of the features of H4 loop also seen in Fig. 17 is the sharp step-down of the desorption branch located in a narrow range of P/P_0 ~0.4–0.5 for nitrogen at temperatures of 77 K. In case of a type IV isotherm, the hysteresis occurs because of capillary condensation when the pore width exceeds ~40 Å [143].

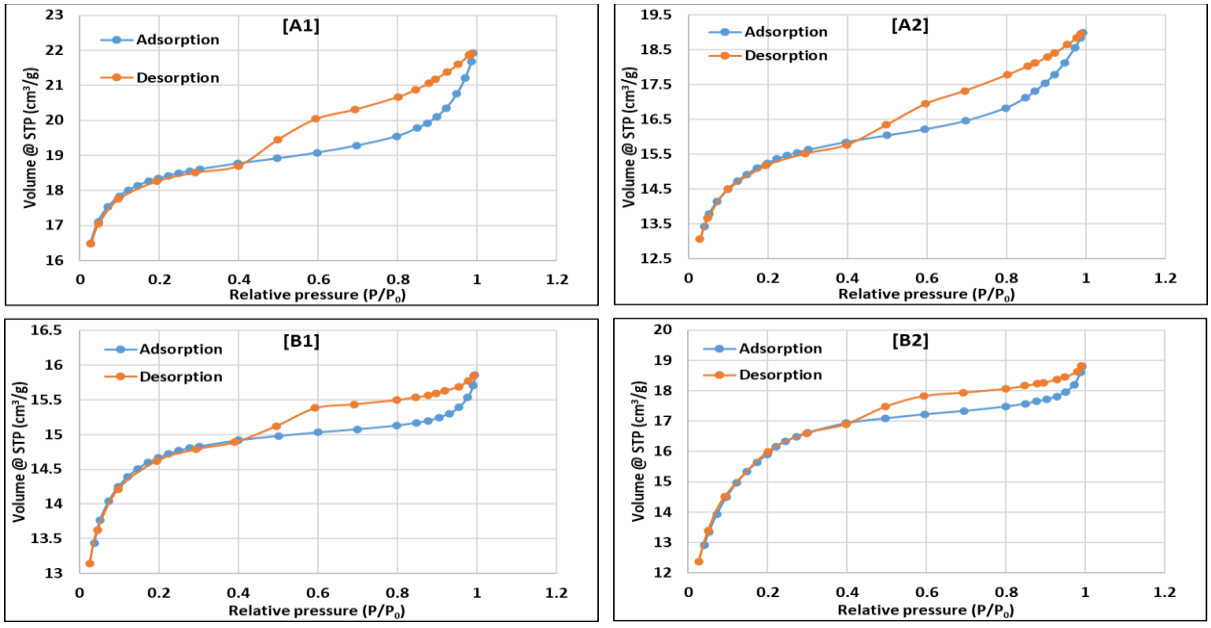

Figure 17. N_2 adsorption/desorption isotherms of [A1] FH biocarbon (IR=0.25), [A2] FH biocarbon (IR=0.50), [B1] AH biocarbon (IR=0.25), and [B2] AH biocarbon (IR=0.50)

The pore size distribution shown in Fig. 18 indicates that all four biocarbon were mostly microporous (<20 Å). High microporous region in biocarbon is desirable in applications like gas-storage/capture [142]. With increase in IR from 0.25 to 0.50, the microporous volume out of total pore volume decreased from 81.6% to 67.8% and 92.6% to 78.5% in FH and AH derived biocarbon, respectively. This decrease in microporous volume with increase in IR could be due to the increased amount of metallic potassium penetration which causes enlargement of carbon matrix and increased porosity [142].

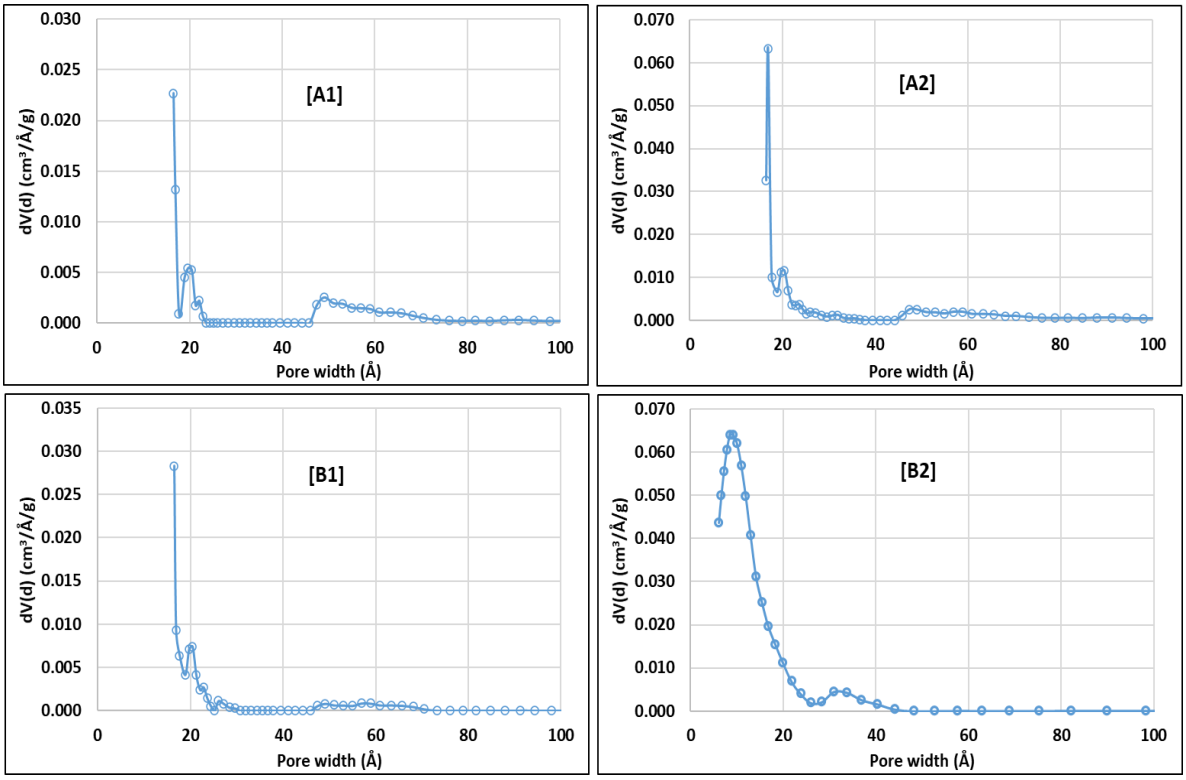

Figure 18. Pore size distribution of [A1] FH biocarbon (IR=0.25), [A2] FH biocarbon (IR=0.50), [B1] AH biocarbon (IR=0.25), and [B2] AH biocarbon (IR=0.50)

BET surface area, total pore volume, and yield for biocarbon produced from FH and AH PESR is shown in Table 10. Despite of the biochemical similarity between FH and AH PESR, there was significant difference in their morphology. The perforated morphology of AH PESR could have caused enhanced metallic potassium penetration compared to FH PESR, resulting in higher BET surface area and total pore volume. This also resulted in lower yield of AH biocarbon at IR=0.5 due to higher decomposition of the PESR.

The elemental and ash content of biocarbon is shown in Table 6. AH PESR had lower ash content compared to FH PESR, this resulted in biocarbon from AH with relatively lower ash. Biocarbon produced without K_2CO_3 (IR=0) had high amount of nitrogen but lacked porosity and active sites. At IR=0.5, both FH and AH biocarbon had 0.6% nitrogen and high porosity which makes it an attractive material for applications including supercapacitor electrodes, CO_2 capture, and catalysts for oxygen reduction reaction. This claim can be further bolstered by the TEM images (Fig. 19) which show continuous branched porous framework of carbon nanosheets and fully interconnected micropores. Wei et al. have reported biocarbon produced from stem bark with similar structure and 1.7% nitrogen doping to have capacitance up to 416 F g^{-1} and CO_2 adsorption up to 6.7 mmol g^{-1} [133]. The magnified TEM images show both FH and AH biocarbon to be highly porous sponge like material with uniform pores. A noticeable difference in the porosity of AH and FH biocarbon is seen which is consistent with the BET analysis. Overall, both FH and AH have their advantages and disadvantages in terms of mode of operation (batch or continuous), reaction severity (acid concentration, temperature, and pressure), and quality of value-added co-products. These factors have an influence on the process economics as well as the scalability. Moving forward, the information generated through this research will be useful in narrowing down the efforts in development of integrated micro-algae biorefinery.

Table 10. BET surface area, total pore volume, and yields for biocarbon produced from FH and AH PESR

	FH			AH		
Impregnation ratio	BET surface area ($m^2\ g^{-1}$)	Total pore volume ($cm^3\ g^{-1}$)	Yield (%)	BET surface area ($m^2\ g^{-1}$)	Total pore volume ($cm^3\ g^{-1}$)	Yield (%)
0	Not detected	Not detected	30.0±1.0	Not detected	Not detected	25.9±1.4
0.25	571.4±80.9	0.35±0.04	29.0±0.3	732.1±35.7	0.40±0.02	25.7±1.3
0.50	711.9±77.9	0.49±0.00	32.5±2.5	1288.5±9.7	0.72±0.00	18.8±0.3

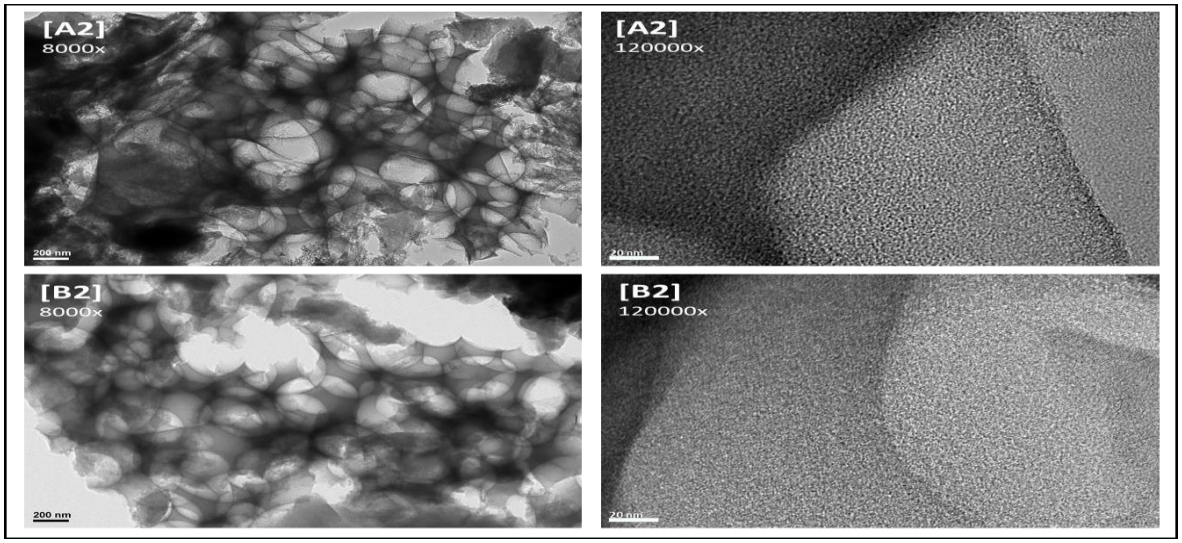

Figure 19. TEM images of [A2] FH biocarbon (IR=0.50) and [B2] AH biocarbon (IR=0.50)

4.4 Conclusions

The biochemicals recovery from micro-algae through two promising fractionation techniques, flash hydrolysis (FH) and acid hydrolysis (AH) was decisively compared. AH (batch mode) had an advantage over FH (continuous mode) in recovering proteins, carbohydrates, and FAME. To utilize micro-algae in entirety, the post extraction solid residue from fractionation process was effectively used to produce biocarbon nanosheets. The BET surface area (FH: 712 $m^2 g^{-1}$ and AH: 1289 $m^2 g^{-1}$), highly microporous structure, and heteroatom containing composition of the renewable biocarbon will make it an attractive material for multiple applications, including supercapacitors, CO_2 capture, and catalysts for oxygen reduction reaction.

4.5 Acknowledgements

This research work was financially supported by the U.S. Department of Energy under Contract No. DE-AC36-08GO28308 with the National Renewable Energy Laboratory, as part of the DOE Office of Energy Efficiency and Renewable Energy, Bioenergy Technologies Office.

CHAPTER 5

RECOMMENDATIONS FOR FUTURE WORKS

In this study, hydrothermal processes were developed, optimized, and applied for extraction and conversion of biomass from various sources to produce bio-chemicals and biofuels with an aim to develop integrated biorefineries. An integrated approach for utilization of biomass in its entirety is believed to be advantageous in making the process economically viable. However, researchers throughout the world have proposed various integrated approaches. Thus, the comparison of these approaches in terms of techno-economics and lifecycle may help in narrowing down the technologies for further investigation and commercialization. While the focus of this research was on producing value-added products effectively, it has also demonstrated some applications of these products. A further investigation directed towards processing these products and its application will help in closing the loop.

As discussed in Chapter 2, the cellulose rich pretreated biomass can be processed using thermochemical and biochemical pathway to produce levulinic acid and fermentable sugars, respectively. Separation, purification, and conversion techniques for these biochemicals to produce end products can be developed further. Since both hydrothermal and biochemical routes have their own advantages and disadvantages, it would be interesting to have techno-economic analysis (TEA) and lifecycle analysis (LCA) for comparison and down selection of the developed pathways.

In Chapter 3, flash hydrolysis (FH) of yeast was discussed for solubilization of proteins. The experiments were done using commercial dry yeast as a model for brewer's spent yeast. The proposed FH technology can be used for processing spent yeast (industrial waste). The spent yeast slurry generated in the industry also has other components like fermentation media,

metabolites, added ingredients like hops etc. The effects of these components on FH of yeast can be researched to bring the technology closer to the commercial settings. Also, unlike high lipid micro-algae, *Saccharomyces cerevisiae* has relatively lower lipids content making it less attractive for biofuel production. For this reason, the solid residue generated through FH of yeast may be directly used for the production of biocarbon material using techniques discussed in Chapter 2 and 4 of this dissertation. The proposed FH technology for recovery of proteins and its application as a nutrient media is an alternative to the widely used enzymatic (biochemical) method for the production of YE. Many advantages and disadvantages of the two techniques were discussed, however, FH may prove to be a good replacement for the traditional method only if it is economically viable and thus it needs further investigation in that direction.

The scaled-up FH technology used in Chapter 3 and 4 was found to have potential application in biomass processing. At the same time, it also had some scope for improvement. All experiments conducted in this research used single pass FH i.e., the biomass slurry was pumped through the reactor only once. Even though the solubilization of biomass components using single pass FH was significant, it could be further improved using multi pass FH i.e., the insoluble biomass residue can be pumped through the reactor multiple times. This could improve solubilization as well as fatty acid methyl ester (FAME) recovery in case of micro-algae. FH technology developed in this research was chemical-free, which makes it a green technology. Adding a small amount of chemicals like acids and bases to the biomass slurry before FH may potentially aid the hydrolysis of biomass. Advantage of chemically aided FH may outweigh its disadvantage of not being chemical free process and thus needs to be evaluated. The pilot FH system used in this research work could process highly concentrated slurry which was not

reported earlier. Nevertheless, the heat and mass transfer in this system can be improved further by modifying the design based on reaction kinetics and simulation using sophisticated software.

Overall, when it comes to hydrothermal technology as observed in this research, solid residue is generated in significant amounts. This solid residue can be effectively used as a low-cost precursor for the production of porous carbon materials which was demonstrated in Chapter 2 and 4. These porous materials with high surface area and volume can be used as a supercapacitor as discussed in Chapter 2. The other unexplored applications could be gas-liquid phase separation, purification of gases, waste-water treatment, catalysis etc. Such materials have the potential to replace existing coal-based carbon used in many industrial applications [144].

REFERENCES

[1] T. Andre, F. Guerra, Renewables 2020 Global Status Report, 2020.

[2] A. Aguilar-Reynosa, A. Romaní, R. Ma. Rodríguez-Jasso, C.N. Aguilar, G. Garrote, H.A. Ruiz, Microwave heating processing as alternative of pretreatment in second-generation biorefinery: An overview, Energy Convers. Manag. 136 (2017) 50–65. https://doi.org/https://doi.org/10.1016/j.enconman.2017.01.004.

[3] S. Fahd, G. Fiorentino, S. Mellino, S. Ulgiati, Cropping bioenergy and biomaterials in marginal land: The added value of the biorefinery concept, Energy. 37 (2012) 79–93. https://doi.org/https://doi.org/10.1016/j.energy.2011.08.023.

[4] H.A. Ruiz, M.A. Cerqueira, H.D. Silva, R.M. Rodríguez-Jasso, A.A. Vicente, J.A. Teixeira, Biorefinery valorization of autohydrolysis wheat straw hemicellulose to be applied in a polymer-blend film, Carbohydr. Polym. 92 (2013) 2154–2162. https://doi.org/https://doi.org/10.1016/j.carbpol.2012.11.054.

[5] A. Demirbas, I. Demirbas, Importance of rural bioenergy for developing countries, Energy Convers. Manag. 48 (2007) 2386–2398. https://doi.org/10.1016/j.enconman.2007.03.005.

[6] H.B. Aditiya, T.M.I. Mahlia, W.T. Chong, H. Nur, A.H. Sebayang, Second generation bioethanol production: A critical review, Renew. Sustain. Energy Rev. 66 (2016) 631–653. https://doi.org/https://doi.org/10.1016/j.rser.2016.07.015.

[7] C.R. Correa, A. Kruse, Supercritical water gasification of biomass for hydrogen production–Review, J. Supercrit. Fluids. 133 (2018) 573–590.

[8] J.K. Saini, R. Saini, L. Tewari, Lignocellulosic agriculture wastes as biomass feedstocks for second-generation bioethanol production: concepts and recent developments, 3 Biotech. 5 (2015) 337–353.

[9] A. Thakkar, K.M. Shell, M. Bertosin, D.D. Rodene, V. Amar, A. Bertucco, R.B. Gupta, R. Shende, S. Kumar, Production of levulinic acid and biocarbon electrode material from corn stover through an integrated biorefinery process, Fuel Process. Technol. (2020) 106644.

[10] FAO, Food wastage footprint: Impacts on natural resources, FAO, 2013. http://www.fao.org/3/i3347e/i3347e.pdf.

[11] FAO, Save Foods: Global Initiative on Food Loss and Waste Reduction, (2014). http://www.fao.org/3/i2776e/i2776e00.pdf.

[12] G.-F. Deng, C. Shen, X.-R. Xu, R.-D. Kuang, Y.-J. Guo, L.-S. Zeng, L.-L. Gao, X. Lin, J.-F. Xie, E.-Q. Xia, Potential of fruit wastes as natural resources of bioactive compounds, Int. J. Mol. Sci. 13 (2012) 8308–8323.

[13] N. Scialabba, O. Jan, C. Tostivint, A. Turbé, C. O'Connor, P. Lavelle, A. Flammini, J. Hoogeveen, M. Iweins, F. Tubiello, L. Peiser, C. Batello, Food Wastage Footprint: Impacts on Natural Resources. Summary Report, 2013.

[14] A.L. Ahmad, N.H.M. Yasin, C.J.C. Derek, J.K. Lim, Microalgae as a sustainable energy source for biodiesel production: A review, Renew. Sustain. Energy Rev. 15 (2011) 584–593. https://doi.org/https://doi.org/10.1016/j.rser.2010.09.018.

[15] Y. Chisti, Biodiesel from microalgae, Biotechnol. Adv. 25 (2007) 294–306. https://doi.org/https://doi.org/10.1016/j.biotechadv.2007.02.001.

[16] T.M. Mata, A.A. Martins, N.S. Caetano, Microalgae for biodiesel production and other applications: A review, Renew. Sustain. Energy Rev. 14 (2010) 217–232. https://doi.org/https://doi.org/10.1016/j.rser.2009.07.020.

[17] A. Demirbaş, Oily Products from Mosses and Algae via Pyrolysis, 2006.

https://doi.org/10.1080/009083190910389.

[18] S. Kumar, Sub- and Supercritical Water Technology for Biofuels, in: J.W. Lee (Ed.), Adv. Biofuels Bioprod., Springer New York, New York, NY, 2013: pp. 147–183. https://doi.org/10.1007/978-1-4614-3348-4_11.

[19] P. Biller, A.B. Ross, S.C. Skill, A. Lea-Langton, B. Balasundaram, C. Hall, R. Riley, C.A. Llewellyn, Nutrient recycling of aqueous phase for microalgae cultivation from the hydrothermal liquefaction process, Algal Res. 1 (2012) 70–76. https://doi.org/https://doi.org/10.1016/j.algal.2012.02.002.

[20] S.P. Slocombe, J.R. Benemann, Microalgal production for biomass and high-value products, CRC Press, 2017.

[21] A.R.K. Gollakota, N. Kishore, S. Gu, A review on hydrothermal liquefaction of biomass, Renew. Sustain. Energy Rev. 81 (2018) 1378–1392. https://doi.org/https://doi.org/10.1016/j.rser.2017.05.178.

[22] H. Shokrkar, S. Ebrahimi, Evaluation of different enzymatic treatment procedures on sugar extraction from microalgal biomass, experimental and kinetic study, Energy. 148 (2018) 258–268.

[23] R.M. Handler, D.R. Shonnard, T.N. Kalnes, F.S. Lupton, Life cycle assessment of algal biofuels: Influence of feedstock cultivation systems and conversion platforms, Algal Res. 4 (2014) 105–115. https://doi.org/https://doi.org/10.1016/j.algal.2013.12.001.

[24] R.E. Davis, D.B. Fishman, E.D. Frank, M.C. Johnson, S.B. Jones, C.M. Kinchin, R.L. Skaggs, E.R. Venteris, M.S. Wigmosta, Integrated evaluation of cost, emissions, and resource potential for algal biofuels at the national scale, Environ. Sci. Technol. 48 (2014) 6035–6042.

[25] S. Kumar, Hydrothermal treatment for biofuels: lignocellulosic biomass to bioethanol, biocrude, and biochar, 2010.

[26] H. Machida, M. Takesue, R.L. Smith Jr, Green chemical processes with supercritical fluids: properties, materials, separations and energy, J. Supercrit. Fluids. 60 (2011) 2–15.

[27] S. Kumar, F. Barla, Sub-and Supercritical Hydrothermal Technology: Industrial Applications, CRC Press, 2019.

[28] B. Hu, S.-H. Yu, K. Wang, L. Liu, X.-W. Xu, Functional carbonaceous materials from hydrothermal carbonization of biomass: an effective chemical process, Dalt. Trans. (2008) 5414–5423.

[29] P.E. Savage, Organic Chemical Reactions in Supercritical Water., Chem. Rev. 99 (1999) 603–622. https://doi.org/10.1021/cr9700989.

[30] M. Watanabe, T. Sato, H. Inomata, R.L. Smith Jr, K. Arai Jr, A. Kruse, E. Dinjus, Chemical reactions of C1 compounds in near-critical and supercritical water, Chem. Rev. 104 (2004) 5803–5822.

[31] P. Krammer, H. Vogel, Hydrolysis of esters in subcritical and supercritical water, J. Supercrit. Fluids. 16 (2000) 189–206.

[32] A. Kruse, E. Dinjus, Hot compressed water as reaction medium and reactant: properties and synthesis reactions, J. Supercrit. Fluids. 39 (2007) 362–380.

[33] Z. Fang, T. Minowa, R.L. Smith, T. Ogi, J.A. Koziński, Liquefaction and Gasification of Cellulose with Na2CO3 and Ni in Subcritical Water at 350 °C, Ind. Eng. Chem. Res. 43 (2004) 2454–2463. https://doi.org/10.1021/ie034146t.

[34] M. Osada, T. Sato, M. Watanabe, M. Shirai, K. Arai, CATALYTIC GASIFICATION OF WOOD BIOMASS IN SUBCRITICAL AND SUPERCRITICAL WATER, Combust. Sci.

Technol. 178 (2006) 537–552. https://doi.org/10.1080/00102200500290807.

[35] H. Schmieder, J. Abeln, N. Boukis, E. Dinjus, A. Kruse, M. Kluth, G. Petrich, E. Sadri, M. Schacht, Hydrothermal gasification of biomass and organic wastes, J. Supercrit. Fluids. 17 (2000) 145–153. https://doi.org/https://doi.org/10.1016/S0896-8446(99)00051-0.

[36] F. Fernand, A. Israel, J. Skjermo, T. Wichard, K.R. Timmermans, A. Golberg, Offshore macroalgae biomass for bioenergy production: Environmental aspects, technological achievements and challenges, Renew. Sustain. Energy Rev. 75 (2017) 35–45. https://doi.org/10.1016/j.rser.2016.10.046.

[37] G. Mukherjee, G. Dhiman, N. Akhtar, Efficient Hydrolysis of Lignocellulosic Biomass: Potential Challenges and Future Perspectives for Biorefineries, in: Bioremediation Sustain. Technol. Clean. Environ., Springer, 2017: pp. 213–237. https://doi.org/10.1007/978-3-319-48439-6_17.

[38] F. Coppola, S. Bastianoni, H. Østergård, Sustainability of bioethanol production from wheat with recycled residues as evaluated by Emergy assessment, Biomass and Bioenergy. 33 (2009) 1626–1642. https://doi.org/10.1016/j.biombioe.2009.08.003.

[39] K.B. Cantrell, J.M. Novak, J.R. Frederick, D.L. Karlen, D.W. Watts, Influence of corn residue harvest management on grain, stover, and energy yields, BioEnergy Res. 7 (2014) 590–597. https://doi.org/10.1007/s12155-014-9433-9.

[40] M.H. Langholtz, B.J. Stokes, L.M. Eaton, 2016 Billion-ton report: Advancing domestic resources for a thriving bioeconomy, Volume 1: Economic availability of feedstock, Oak Ridge Natl. Lab. Oak Ridge, Tennessee, Manag. by UT-Battelle, LLC US Dep. Energy. 2016 (2016) 1–411.

[41] S. Malherbe, T.E. Cloete, Lignocellulose biodegradation: fundamentals and applications, Rev. Environ. Sci. Biotechnol. 1 (2002) 105–114. https://doi.org/10.1023/A:1020858910646.

[42] S. Kumar, U. Kothari, L. Kong, Y.Y. Lee, R.B. Gupta, Hydrothermal pretreatment of switchgrass and corn stover for production of ethanol and carbon microspheres, Biomass and Bioenergy. 35 (2011) 956–968. https://doi.org/10.1016/j.biombioe.2010.11.023.

[43] H. Yu, Y. Xu, J. Hou, Y. Ni, S. Liu, Y. Liu, S. Yu, S. Nie, Q. Wu, C. Wu, Efficient fractionation of corn stover for biorefinery using a sustainable pathway, ACS Sustain. Chem. Eng. 8 (2020) 3454–3464. https://doi.org/10.1021/acssuschemeng.9b07791.

[44] D.W. Rackemann, W.O.S. Doherty, The conversion of lignocellulosics to levulinic acid, Biofuels, Bioprod. Biorefining. 5 (2011) 198–214. https://doi.org/10.1002/bbb.267.

[45] D. Licursi, C. Antonetti, S. Fulignati, S. Vitolo, M. Puccini, E. Ribechini, L. Bernazzani, A.M.R. Galletti, In-depth characterization of valuable char obtained from hydrothermal conversion of hazelnut shells to levulinic acid, Bioresour. Technol. 244 (2017) 880–888. https://doi.org/10.1016/j.biortech.2017.08.012.

[46] S. Rivas, A.M. Raspolli-Galletti, C. Antonetti, V. Santos, J.C. Parajó, Sustainable conversion of Pinus pinaster wood into biofuel precursors: A biorefinery approach, Fuel. 164 (2016) 51–58. https://doi.org/10.1016/j.fuel.2015.09.085.

[47] C. Chang, P. Cen, X. Ma, Levulinic acid production from wheat straw, Bioresour. Technol. 98 (2007) 1448–1453. https://doi.org/https://doi.org/10.1016/j.biortech.2006.03.031.

[48] A.A. Efremov, G.G. Pervyshina, B.N. Kuznetsov, Thermocatalytic transformations of wood and cellulose in the presence of HCl, HBr, and H2SO4, Chem. Nat. Compd. 33

(1997) 84–88. https://doi.org/10.1007/BF02273932.

[49] L. Yan, N. Yang, H. Pang, B. Liao, Production of Levulinic Acid from Bagasse and Paddy Straw by Liquefaction in the Presence of Hydrochloride Acid, CLEAN – Soil, Air, Water. 36 (2008) 158–163. https://doi.org/10.1002/clen.200700100.

[50] W. Chen, H. Hu, Q. Cai, S. Zhang, Synergistic effects of furfural and sulfuric acid on the decomposition of levulinic acid, Energy & Fuels. 34 (2020) 2238–2245. https://doi.org/10.1021/acs.energyfuels.9b03971.

[51] L.G. Covinich, N.M. Clauser, F.E. Felissia, M.E. Vallejos, M.C. Area, The challenge of converting biomass polysaccharides into levulinic acid through heterogeneous catalytic processes, Biofuels, Bioprod. Biorefining. 14 (2020) 417–445. https://doi.org/10.1002/bbb.2062.

[52] T. Runge, C. Zhang, Two-Stage Acid-Catalyzed Conversion of Carbohydrates into Levulinic Acid, Ind. Eng. Chem. Res. 51 (2012) 3265–3270. https://doi.org/10.1021/ie2021619.

[53] E.S. Lopes, J.F. Leal Silva, E.C. Rivera, A.P. Gomes, M.S. Lopes, R. Maciel Filho, L.P. Tovar, Challenges to Levulinic Acid and Humins Valuation in the Sugarcane Bagasse Biorefinery Concept, BioEnergy Res. (2020) 1–18. https://doi.org/10.1007/s12155-020-10124-9.

[54] C. Antonetti, D. Licursi, S. Fulignati, G. Valentini, A.M. Raspolli Galletti, New frontiers in the catalytic synthesis of levulinic acid: from sugars to raw and waste biomass as starting feedstock, Catalysts. 6 (2016) 196. https://doi.org/10.3390/catal6120196.

[55] B. V Timokhin, V.A. Baransky, G.D. Eliseeva, Levulinic acid in organic synthesis, Russ. Chem. Rev. 68 (1999) 73. https://doi.org/10.1070/RC1999v068n01ABEH000381.

[56] D.J. Hayes, S. Fitzpatrick, M.H.B. Hayes, J.R.H. Ross, The biofine process–production of levulinic acid, furfural, and formic acid from lignocellulosic feedstocks, Biorefineries–Industrial Process. Prod. 1 (2006) 139–164.

[57] H. Jeong, S.-K. Jang, C.-Y. Hong, S.-H. Kim, S.-Y. Lee, S.M. Lee, J.W. Choi, I.-G. Choi, Levulinic acid production by two-step acid-catalyzed treatment of Quercus mongolica using dilute sulfuric acid, Bioresour. Technol. 225 (2017) 183–190. https://doi.org/10.1016/j.biortech.2016.11.063.

[58] Y. Muranaka, T. Suzuki, H. Sawanishi, I. Hasegawa, K. Mae, Effective production of levulinic acid from biomass through pretreatment using phosphoric acid, hydrochloric acid, or ionic liquid, Ind. Eng. Chem. Res. 53 (2014) 11611–11621. https://doi.org/10.1021/ie501811x.

[59] M.J. Díaz, C. Cara, E. Ruiz, I. Romero, M. Moya, E. Castro, Hydrothermal pre-treatment of rapeseed straw, Bioresour. Technol. 101 (2010) 2428–2435. https://doi.org/10.1016/j.biortech.2009.10.085.

[60] T.-A. Hsu, Pretreatment of biomass. In, Wyman, CE (Ed.), editor. Handbook on Bioethanol, production and utilization, (1996).

[61] R. Jaswal, A. Shende, W. Nan, V. Amar, R. Shende, Hydrothermal Liquefaction and Photocatalytic Reforming of Pinewood (Pinus ponderosa)-Derived Acid Hydrolysis Residue for Hydrogen and Bio-oil Production, Energy & Fuels. 33 (2019) 6454–6462. https://doi.org/10.1021/acs.energyfuels.9b01071.

[62] Y. Sun, J. Cheng, Hydrolysis of lignocellulosic materials for ethanol production: a review, Bioresour. Technol. 83 (2002) 1–11. https://doi.org/10.1016/S0960-8524(01)00212-7.

[63] O. Bobleter, Hydrothermal degradation of polymers derived from plants, Prog. Polym.

Sci. 19 (1994) 797–841. https://doi.org/https://doi.org/10.1016/0079-6700(94)90033-7.

[64] A. Hendriks, G. Zeeman, Pretreatments to enhance the digestibility of lignocellulosic biomass, Bioresour. Technol. 100 (2009) 10–18. https://doi.org/10.1016/j.biortech.2008.05.027.

[65] K.L. Kohlmann, A. Sarikaya, P.J. Westgate, J. Weil, A. Velayudhan, R. Hendrickson, M.R. Ladisch, Enhanced enzyme activities on hydrated lignocellulosic substrates, in: ACS Publications, 1995. https://pubs.acs.org/doi/abs/10.1021/bk-1995-0618.ch015.

[66] R.S. Laxman, A.H. Lachke, Bioethanol lignocellulosic biomass, Handb. Plant-Based Biofuels. (2009) 121–139.

[67] N. Mosier, R. Hendrickson, N. Ho, M. Sedlak, M.R. Ladisch, Optimization of pH controlled liquid hot water pretreatment of corn stover, Bioresour. Technol. 96 (2005) 1986–1993. https://doi.org/10.1016/j.biortech.2005.01.013.

[68] A. Thakkar, S. Kumar, Hydrothermal Carbonization for Producing Carbon Materials, in: Sub-and Supercrit. Hydrothermal Technol., CRC Press, 2019: pp. 67–83.

[69] J. Weil, M. Brewer, R. Hendrickson, A. Sarikaya, M.R. Ladisch, Continuous pH monitoring during pretreatment of yellow poplar wood sawdust by pressure cooking in water, in: Biotechnol. Fuels Chem., Springer, 1998: pp. 99–111. https://doi.org/10.1007/978-1-4612-1814-2_10.

[70] C. Liu, C.E. Wyman, The Effect of Flow Rate of Compressed Hot Water on Xylan, Lignin, and Total Mass Removal from Corn Stover, Ind. Eng. Chem. Res. 42 (2003) 5409–5416. https://doi.org/10.1021/ie030458k.

[71] T. Rogalinski, T. Ingram, G. Brunner, Hydrolysis of lignocellulosic biomass in water under elevated temperatures and pressures, J. Supercrit. Fluids. 47 (2008) 54–63.

https://doi.org/10.1016/j.supflu.2008.05.003.

[72] A. González, E. Goikolea, J.A. Barrena, R. Mysyk, Review on supercapacitors: Technologies and materials, Renew. Sustain. Energy Rev. 58 (2016) 1189–1206. https://doi.org/https://doi.org/10.1016/j.rser.2015.12.249.

[73] F. Fu, D. Yang, W. Zhang, H. Wang, X. Qiu, Green self-assembly synthesis of porous lignin-derived carbon quasi-nanosheets for high-performance supercapacitors, Chem. Eng. J. 392 (2020) 123721. https://doi.org/https://doi.org/10.1016/j.cej.2019.123721.

[74] L. Pang, B. Zou, X. Han, L. Cao, W. Wang, Y. Guo, One-step synthesis of high-performance porous carbon from corn starch for supercapacitor, Mater. Lett. 184 (2016) 88–91. https://doi.org/10.1016/j.matlet.2016.07.147.

[75] H. Jin, X. Wang, Y. Shen, Z. Gu, A high-performance carbon derived from corn stover via microwave and slow pyrolysis for supercapacitors, J. Anal. Appl. Pyrolysis. 110 (2014) 18–23. https://doi.org/10.1016/j.jaap.2014.07.010.

[76] L. Wang, G. Mu, C. Tian, L. Sun, W. Zhou, P. Yu, J. Yin, H. Fu, Porous Graphitic Carbon Nanosheets Derived from Cornstalk Biomass for Advanced Supercapacitors, ChemSusChem. 6 (2013) 880–889. https://doi.org/10.1002/cssc.201200990.

[77] T. Mitravinda, K. Nanaji, S. Anandan, A. Jyothirmayi, V.S.K. Chakravadhanula, C.S. Sharma, T.N. Rao, Facile Synthesis of Corn Silk Derived Nanoporous Carbon for an Improved Supercapacitor Performance, J. Electrochem. Soc. 165 (2018) A3369–A3379. https://doi.org/10.1149/2.0621814jes.

[78] S. Song, F. Ma, G. Wu, D. Ma, W. Geng, J. Wan, Facile self-templating large scale preparation of biomass-derived 3D hierarchical porous carbon for advanced supercapacitors, J. Mater. Chem. A. 3 (2015) 18154–18162.

https://doi.org/10.1039/C5TA04721H.

[79] A. Sluiter, B. Hames, Determination of structural carbohydrates and lignin in biomass. Technical Report NREL/TP-510-42618. Sluiter, A., Ruiz, R., Scarlata, C., Sluiter, J., & Templeton, D.(2008). Determination of extractives in biomass. Technical Report NREL/TP-510-42619. Sper, Lina Fernanda Ballesteros Giraldo. 27 (2016) 74.

[80] M.G. Resch, J.O. Baker, S.R. Decker, Low Solids Enzymatic Saccharification of Lignocellulosic Biomass:., National Renewable Energy Laboratory Golden, CO, 2015.

[81] X. Zheng, Z. Zhi, X. Gu, X. Li, R. Zhang, X. Lu, Kinetic study of levulinic acid production from corn stalk at mild temperature using FeCl3 as catalyst, Fuel. 187 (2017) 261–267. https://doi.org/https://doi.org/10.1016/j.fuel.2016.09.019.

[82] B. Girisuta, B. Danon, R. Manurung, L. Janssen, H.J. Heeres, Experimental and kinetic modelling studies on the acid-catalysed hydrolysis of the water hyacinth plant to levulinic acid, Bioresour. Technol. 99 (2008) 8367–8375. https://doi.org/10.1016/j.biortech.2008.02.045.

[83] T.A. McMurray, J.A. Byrne, P.S.M. Dunlop, J.G.M. Winkelman, B.R. Eggins, E.T. McAdams, Intrinsic kinetics of photocatalytic oxidation of formic and oxalic acid on immobilised TiO2 films, Appl. Catal. A Gen. 262 (2004) 105–110. https://doi.org/10.1016/j.apcata.2003.11.013.

[84] J. Zerbe, A. Baker, Investigation of fundamentals of two-stage, dilute sulfuric acid hydrolysis of wood, Symp. Pap. - Energy from Biomass Wastes. (1987) 927–947.

[85] G. Garrote, H. Dominguez, J.C. Parajo, Hydrothermal processing of lignocellulosic materials, Holz Als Roh-Und Werkst. 57 (1999) 191–202.

[86] M. Heitz, F. Carrasco, M. Rubio, G. Chauvette, E. Chornet, L. Jaulin, R.P. Overend,

Generalized correlations for the aqueous liquefaction of lignocellulosics, Can. J. Chem. Eng. 64 (1986) 647–650. https://doi.org/10.1002/cjce.5450640416.

[87] S. Kang, J. Fu, G. Zhang, From lignocellulosic biomass to levulinic acid: A review on acid-catalyzed hydrolysis, Renew. Sustain. Energy Rev. 94 (2018) 340–362. https://doi.org/10.1016/j.rser.2018.06.016.

[88] G.V. Marson, R.J.S. de Castro, M.-P. Belleville, M.D. Hubinger, Spent brewer's yeast as a source of high added value molecules: a systematic review on its characteristics, processing and potential applications, World J. Microbiol. Biotechnol. 36 (2020) 1–22.

[89] G.S. Menegazzi, W.M. Ingledew, Heat processing of spent brewer's yeast, J. Food Sci. 45 (1980) 182–186.

[90] W. Lamoolphak, M. Goto, M. Sasaki, M. Suphantharika, C. Muangnapoh, C. Prommuag, A. Shotipruk, Hydrothermal decomposition of yeast cells for production of proteins and amino acids, J. Hazard. Mater. 137 (2006) 1643–1648. https://doi.org/https://doi.org/10.1016/j.jhazmat.2006.05.029.

[91] E. Vieira, T. Brandão, I.M. Ferreira, Evaluation of brewer's spent yeast to produce flavor enhancer nucleotides: influence of serial repitching, J. Agric. Food Chem. 61 (2013) 8724–8729.

[92] E.F. Vieira, J. Carvalho, E. Pinto, S. Cunha, A.A. Almeida, I.M. Ferreira, Nutritive value, antioxidant activity and phenolic compounds profile of brewer's spent yeast extract, J. Food Compos. Anal. 52 (2016) 44–51.

[93] L. Narziß, W. Back, M. Gastl, M. Zarnkow, Abriss der Bierbrauerei, John Wiley & Sons, 2017.

[94] D.E. Quain, Yeast supply and propagation in brewing, in: Brewing, Elsevier, 2006: pp.

167–182.

[95] J. Berlowska, M. Dudkiewicz-Kołodziejska, E. Pawlikowska, K. Pielech-Przybylska, M. Balcerek, A. Czysowska, D. Kregiel, Utilization of post-fermentation yeasts for yeast extract production by autolysis: the effect of yeast strain and saponin from Quillaja saponaria, J. Inst. Brew. 123 (2017) 396–401.

[96] P.J. Reeds, Dispensable and indispensable amino acids for humans, J. Nutr. 130 (2000) 1835S-1840S.

[97] M. Amorim, J.O. Pereira, D. Gomes, C.D. Pereira, H. Pinheiro, M. Pintado, Nutritional ingredients from spent brewer's yeast obtained by hydrolysis and selective membrane filtration integrated in a pilot process, J. Food Eng. 185 (2016) 42–47. https://doi.org/10.1016/j.jfoodeng.2016.03.032.

[98] G.M. Caballero-Córdoba, V.C. Sgarbieri, Nutritional and toxicological evaluation of yeast (Saccharomyces cerevisiae) biomass and a yeast protein concentrate, J. Sci. Food Agric. 80 (2000) 341–351.

[99] B. Podpora, F. Swiderski, A. Sadowska, A. Piotrowska, R. Rakowska, Spent brewer's yeast autolysates as a new and valuable component of functional food and dietary supplements, J. Food Process. Technol. 6 (2015) 1.

[100] R. Dhakal, V.K. Bajpai, K.-H. Baek, Production of GABA (γ-aminobutyric acid) by microorganisms: a review, Brazilian J. Microbiol. 43 (2012) 1230–1241.

[101] S. Fuke, S. Konosu, Taste-active components in some foods: a review of Japanese research, Physiol. Behav. 49 (1991) 863–868.

[102] P. Münch, P. Schieberle, Quantitative studies on the formation of key odorants in thermally treated yeast extracts using stable isotope dilution assays, J. Agric. Food Chem.

46 (1998) 4695–4701.

[103] F.F. Jacob, M. Hutzler, F.-J. Methner, Comparison of various industrially applicable disruption methods to produce yeast extract using spent yeast from top-fermenting beer production: influence on amino acid and protein content, Eur. Food Res. Technol. 245 (2019) 95–109.

[104] H.J. Chae, H. Joo, M.-J. In, Utilization of brewer's yeast cells for the production of food-grade yeast extract. Part 1: effects of different enzymatic treatments on solid and protein recovery and flavor characteristics, Bioresour. Technol. 76 (2001) 253–258.

[105] G.P. Casey, C.A. Magnus, W.M. Ingledew, High-gravity brewing: effects of nutrition on yeast composition, fermentative ability, and alcohol production, Appl. Environ. Microbiol. 48 (1984) 639–646.

[106] J. Geciova, D. Bury, P. Jelen, Methods for disruption of microbial cells for potential use in the dairy industry—a review, Int. Dairy J. 12 (2002) 541–553.

[107] W.M. Ingledew, F.W. Sosulski, C.A. Magnus, An assessment of yeast foods and their utility in brewing and enology, J. Am. Soc. Brew. Chem. 44 (1986) 166–170.

[108] S. Procopio, D. Krause, T. Hofmann, T. Becker, Significant amino acids in aroma compound profiling during yeast fermentation analyzed by PLS regression, LWT-Food Sci. Technol. 51 (2013) 423–432.

[109] N.I. Belousova, S. V Gordienko, V.K. Eroshin, Influence of autolysis conditions on the properties of amino-acid mixtures produced by ethanol-assimilating yeast, Appl. Biochem. Microbiol. 31 (1995) 391–395.

[110] R. Kollár, E. Šturdík, V. Farkaš, Induction and acceleration of yeast lysis by addition of fresh yeast autolysate, Biotechnol. Lett. 13 (1991) 543–546.

[111] D. Knorr, K.J. Shetty, L.F. Hood, J.E. Kinsella, An enzymatic method fob yeast autolysis, J. Food Sci. 44 (1979) 1362–1365.

[112] R. Sommer, Yeast extracts: production, properties and components, Food Aust. 50 (1998) 181–183.

[113] K.S. Kim, H.S. Yun, Production of soluble β-glucan from the cell wall of Saccharomyces cerevisiae, Enzyme Microb. Technol. 39 (2006) 496–500.

[114] M.B. Esteban, A.J. García, P. Ramos, M.C. Márquez, Kinetics of amino acid production from hog hair by hydrolysis in sub-critical water, J. Supercrit. Fluids. 46 (2008) 137–141.

[115] J.L. Garcia-Moscoso, A. Teymouri, S. Kumar, Kinetics of peptides and arginine production from microalgae (Scenedesmus sp.) by flash hydrolysis, Ind. Eng. Chem. Res. 54 (2015) 2048–2058.

[116] J.L. Garcia-Moscoso, W. Obeid, S. Kumar, P.G. Hatcher, Flash hydrolysis of microalgae (Scenedesmus sp.) for protein extraction and production of biofuels intermediates, J. Supercrit. Fluids. 82 (2013) 183–190.

[117] S.M. Changi, J.L. Faeth, N. Mo, P.E. Savage, Hydrothermal reactions of biomolecules relevant for microalgae liquefaction, Ind. Eng. Chem. Res. 54 (2015) 11733–11758.

[118] C. Torri, L. Garcia Alba, C. Samori, D. Fabbri, D.W.F. Brilman, Hydrothermal treatment (HTT) of microalgae: detailed molecular characterization of HTT oil in view of HTT mechanism elucidation, Energy & Fuels. 26 (2012) 658–671.

[119] K.A. Thompson, R.S. Summers, S.M. Cook, Development and experimental validation of the composition and treatability of a new synthetic bathroom greywater (SynGrey), Environ. Sci. Water Res. Technol. 3 (2017) 1120–1131.

[120] L.M.L. Laurens, N. Nagle, R. Davis, N. Sweeney, S. Van Wychen, A. Lowell, P.T.

Pienkos, Acid-catalyzed algal biomass pretreatment for integrated lipid and carbohydrate-based biofuels production, Green Chem. 17 (2015) 1145–1158.

[121] T. Dong, E.P. Knoshaug, R. Davis, L.M.L. Laurens, S. Van Wychen, P.T. Pienkos, N. Nagle, Combined algal processing: A novel integrated biorefinery process to produce algal biofuels and bioproducts, Algal Res. 19 (2016) 316–323.

[122] M. Wiatrowski, R. Davis, Algal Biomass Conversion to Fuels via Combined Algae Processing (CAP): 2020 State of Technology and Future Research, National Renewable Energy Lab.(NREL), Golden, CO (United States), 2021.

[123] R. Davis, M. Wiatrowski, Algal Biomass Conversion to Fuels via Combined Algae Processing (CAP): 2019 State of Technology and Future Research, National Renewable Energy Lab.(NREL), Golden, CO (United States), 2020.

[124] A. Teymouri, K.J. Adams, T. Dong, S. Kumar, Evaluation of lipid extractability after flash hydrolysis of algae, Fuel. 224 (2018) 23–31.

[125] R. Davis, M. Biddy, S. Jones, Algal lipid extraction and upgrading to hydrocarbons technology pathway, National Renewable Energy Lab.(NREL), Golden, CO (United States), 2013.

[126] R. Ranjith Kumar, P. Hanumantha Rao, M. Arumugam, Lipid extraction methods from microalgae: a comprehensive review, Front. Energy Res. 2 (2015) 61.

[127] T. Dong, S. Van Wychen, N. Nagle, P.T. Pienkos, L.M.L. Laurens, Impact of biochemical composition on susceptibility of algal biomass to acid-catalyzed pretreatment for sugar and lipid recovery, Algal Res. 18 (2016) 69–77.

[128] A.P. Pereira, T. Dong, E.P. Knoshaug, N. Nagle, R. Spiller, B. Panczak, C.J. Chuck, P.T. Pienkos, An alternative biorefinery approach to address microalgal seasonality: blending

with spent coffee grounds, Sustain. Energy Fuels. 4 (2020) 3400–3408.

[129] R. Davis, M. Wiatrowski, C. Kinchin, D. Humbird, Conceptual Basis and Techno-Economic Modeling for Integrated Algal Biorefinery Conversion of Microalgae to Fuels and Products. 2019 NREL TEA Update: Highlighting Paths to Future Cost Goals via a New Pathway for Combined Algal Processing, National Renewable Energy Lab.(NREL), Golden, CO (United States), 2020.

[130] A. Thakkar, E. Barbera, E. Sforza, A. Bertucco, R. Davis, S. Kumar, Flash hydrolysis of yeast (Saccharomyces cerevisiae) for protein recovery, J. Supercrit. Fluids. 173 (2021) 105240.

[131] Y.-M. Chang, W.-T. Tsai, M.-H. Li, Characterization of activated carbon prepared from chlorella-based algal residue, Bioresour. Technol. 184 (2015) 344–348.

[132] T. Dong, E.P. Knoshaug, P.T. Pienkos, L.M.L. Laurens, Lipid recovery from wet oleaginous microbial biomass for biofuel production: a critical review, Appl. Energy. 177 (2016) 879–895.

[133] T. Wei, Q. Zhang, X. Wei, Y. Gao, H. Li, A facile and low-cost route to heteroatom doped porous carbon derived from broussonetia papyrifera bark with excellent supercapacitance and CO 2 capture performance, Sci. Rep. 6 (2016) 1–9.

[134] R. Wang, T. Zhou, H. Li, H. Wang, H. Feng, J. Goh, S. Ji, Nitrogen-rich mesoporous carbon derived from melamine with high electrocatalytic performance for oxygen reduction reaction, J. Power Sources. 261 (2014) 238–244.

[135] I.I. Gurten, M. Ozmak, E. Yagmur, Z. Aktas, Preparation and characterisation of activated carbon from waste tea using K2CO3, Biomass and Bioenergy. 37 (2012) 73–81.

[136] E.P. Knoshaug, T. Dong, R. Spiller, N. Nagle, P.T. Pienkos, Pretreatment and

fermentation of salt-water grown algal biomass as a feedstock for biofuels and high-value biochemicals, Algal Res. 36 (2018) 239–248.

[137] A. Sluiter, B. Hames, R. Ruiz, C. Scarlata, J. Sluiter, D. Templeton, Determination of sugars, byproducts, and degradation products in liquid fraction process samples, Golden Natl. Renew. Energy Lab. 11 (2006) 65–71.

[138] S. Van Wychen, L.M.L. Laurens, Determination of total carbohydrates in algal biomass: laboratory analytical procedure (LAP), National Renewable Energy Lab.(NREL), Golden, CO (United States), 2016.

[139] L.M. Wendt, B.D. Wahlen, E.P. Knoshaug, N.J. Nagle, T. Dong, R. Spiller, B. Panczak, S. Van Wychen, T.A. Dempster, H. Gerken, Anaerobic Storage and Conversion of Microalgal Biomass to Manage Seasonal Variation in Cultivation, ACS Sustain. Chem. Eng. 8 (2020) 13310–13317.

[140] S. Van Wychen, K. Ramirez, L.M.L. Laurens, Determination of total lipids as fatty acid methyl esters (FAME) by in situ transesterification: laboratory analytical procedure (LAP), National Renewable Energy Lab.(NREL), Golden, CO (United States), 2016.

[141] S. Van Wychen, S.M. Rowland, K.C. Lesco, P. V Shanta, T. Dong, L.M.L. Laurens, Advanced mass balance characterization and fractionation of algal biomass composition, J. Appl. Phycol. 33 (2021) 2695–2708.

[142] J. Romanos, M. Beckner, T. Rash, L. Firlej, B. Kuchta, P. Yu, G. Suppes, C. Wexler, P. Pfeifer, Nanospace engineering of KOH activated carbon, Nanotechnology. 23 (2011) 15401.

[143] M. Thommes, K. Kaneko, A. Neimark, J. Olivier, F. Rodriguez-Reinoso, J. Rouquerol, K. Sing, Physisorption of gases, with special reference to the evaluation of surface area and

pore size distribution (IUPAC Technical Report), Pure Appl. Chem. 87 (2015). https://doi.org/10.1515/pac-2014-1117.

[144] R. Aravindhan, J.R. Rao, B.U. Nair, Preparation and characterization of activated carbon from marine macro-algal biomass, J. Hazard. Mater. 162 (2009) 688–694.

APPENDICES

APPENDIX A: OPERATION, TROUBLESHOOTING, AND SAFETY MEASURES FOR PILOT FLASH HYDROLYSIS UNIT

1. Start-up and operation

1. Ensure all units are plugged into the appropriate power supply.
    a. Chilling unit: 230V outlet
    b. LEWA pump: 115V outlet
    - Pump turns on automatically when plugged in, use a power strip as an on/off switch.
    c. Induction heat power supply: 230V outlet
    d. Induction heat digital display: 115V outlet
2. Turn on chilling unit: Must be turned on prior to induction heat power supply to prevent its overheating.
3. Prime Lewa pump: If the pump has not been used for several days, priming may be necessary.
    a. To prime the pump, close the inlet valve so water is only pulled from the calibration column (shown in picture below).
    b. Ensure pressure regulators are set to zero as not to increase pressure created by the pump.
    c. Turn on the pump and allow distilled (DI) water to be drawn from the calibration column that is elevated above the pump inlet.
    - Ensure no air pockets or bubbles are formed. Pump outlet may have to be disconnected from the system for this to occur.

4. Once the pump is primed, flow of DI water needs to be slowly transitioned from the calibration column to slurry reservoir (elevated above pump level).
    a. This can be done by slowly opening the valves to allow slurry to flow from the reservoir using the two valves shown in picture below.
    b. If the pump does nor need priming, start pumping slurry directly.
5. Set back pressure regulator (BPR) to operation pressure: This is done by adjusting the air regulator on the compressed air cylinder that is connected to the dome loaded BPR.
    a. Verify that the pressure gauge at the pump outlet reads required operating pressure. If not, adjust the compressed air regulator.
6. After reaching operating pressure, ensure flow is continuous from the outlet of the dome loaded BPR.
7. Once flow is established the induction heating can be turned on.
    a. First turn both switches on the power supply.
    b. Once the power supply is on you can access the digital display.
    - Select appropriate heating rate/ramp up time and final temperature.
    - Parameters can be adjusted via the digital display as need. Please refer to the manual to do so.
8. Allow system to reach desired temperature.
9. Watch pump outlet pressure to check for clogging. If pressure stays elevated above operating pressure a clog has likely occurred, and system should be shut down.
10. If the flow is smooth and temperature/pressure are stable, start collecting the hydrolysate in an appropriate container at the outlet.

2. Shutdown

1. Shut off induction heating using the digital display.
2. Allow system to cool to <50°C.
3. Reduce the back pressure slowly to 0, using air regulator.
4. Switch flow from slurry reservoir to DI water reservoir.
5. Allow water to flow through the system until slurry is cleared.
6. Turn off pump.

3. Troubleshooting

Symptom (commonly observed)	Possible cause	Remedy
No flow at the outlet	1. Improper priming 2. Inlet line is not submerged in fluid 3. Clogging in the line or reactor 4. Clogging in BPR 5. Slurry too concentrated or viscous 6. Pump check valve dirty or damaged	1. Prime the pump using calibration column 2. Ensure fluid level in reservoir is above the inlet line 3. Dismantle and clean the lines and reactor 4. Unclog the BPR by back flushing 5. Dilute the slurry 6. Clean the inlet and outlet check valve (replace if cleaning doesn't help)
Overheated reactor (reddening)	1. Insufficient or discontinuous flow	1. Dismantle and clean the lines and reactor; Unclog the BPR by back flushing; Clean the inlet and outlet check valve (replace if cleaning doesn't help)
Air in outlet line	1. BPR O-ring misplaced 2. Ruptured BPR diaphragm	1. Reposition O-ring (replace if damaged)

		2. Replace BPR diaphragm
Temperature fluctuation around set point	1. Insufficient or discontinuous flow 2. High pulsation in flow 3. Improper PID controller setting	1. Dismantle and clean the lines and reactor; Unclog the BPR by back flushing; Clean the inlet and outlet check valve (replace if cleaning doesn't help) 2. Check pressure in pulsation dampener and refill if required 3. Change PID controller setting (trial and error)
Insufficient pump outlet pressure	1. Pump check valve dirty or damaged	1. Clean the inlet and outlet check valve (replace if cleaning doesn't help)
Note: Before using the above remedies make sure routine maintenance for pump and chiller is done. Refer to instrument manuals for other uncommon symptoms.		

4. Safety measures

1. Do not touch any of the electrical connections or hot surfaces with bare hands.
2. Always use personal protective equipment (PPE) while operating the unit.
3. Use strainer to remove any large suspended particles or clumps in the slurry to protect the pump.

4. Before operation, check the accuracy of the reactor thermocouple using a reference thermocouple.
5. Be watchful of the steam venting out from the weep hole during the heating and cooling of the reactor.
6. Use the emergency stop on the induction heat power supply if reddening of reactor is observed due to overheating.
7. Always set the high temperature cutoff in the induction heat digital display.
8. Do not exceed the max pressure limit for any of the component in the system.

VITA

Anuj Hemant Thakkar

EDUCATION

Doctor of Philosophy, Civil and Environmental Engineering **December 2021**
Old Dominion University, Norfolk, USA
Dissertation: *Hydrothermal Processes for Extraction and Conversion of Biomass to Produce Biofuels and Value-Added Products*

Master of Science, Biochemical Engineering **July 2014**
Manipal University, Manipal, India
Thesis: *Hydrothermal Liquefaction of Biomass*

Bachelor of Science, Biotechnology **July 2012**
University of Pune, Pune, India
Thesis: *Commercialization and Standardization of Biogas Plant*

RESEARCH PAPERS AND BOOK CHAPATERS

- Comparative study of flash and acid hydrolysis of micro-algae for the recovery of biochemicals and production of porous biocarbon nanosheets (**Anuj Thakkar**, Philip T. Pienkos, Nick Nagle, Tao Dong, Jacob Kruger, and Sandeep Kumar), Biomass Conversion and Biorefinery, 2021 (under review).
- Flash hydrolysis of yeast (Saccharomyces cerevisiae) for protein recovery (**Anuj Thakkar**, Elena Barbera, Eleonora Sforza, Alberto Bertucco, Ryan Davis, and Sandeep Kumar), Journal of Supercritical Fluids, 2021.
- Hydrothermal liquefaction (HTL) processing of unhydrolyzed solids (UHS) for hydrochar and its use for asymmetric supercapacitors with mixed (Mn, Ti)-Perovskite oxides (Vinod Amar, Joseph Houck, Bharath Maddipudi, Trevor Penrod, Katelyn Shell, **Anuj Thakkar**, Anuradha Shende, Sergio Hernandez, Sandeep Kumar, Ram Gupta, and Rajesh Shende), Renewable Energy, 2021.
- Supercapacitor performance of biocarbon produced from non-catalytic hydrothermal liquefaction of lignin-rich biomass (Katelyn Shell, Dylan Rodene, Vinod Amar, **Anuj Thakkar**, Bharath Maddipudi, Sandeep Kumar, Rajesh Shende, and Ram Gupta), Bioresource Technology Reports, 2021.
- Production of levulinic acid and biocarbon electrode material from corn stover through an integrated biorefinery process (**Anuj Thakkar**, Katelyn Shell, Martino Bertosin, Dylan Rodene, Vinod Amar, Alberto Bertucco, Ram Gupta, Rajesh Shende, and Sandeep Kumar), Fuel Processing Technology, 2021.
- Hydrothermal carbonization for producing carbon materials (**Anuj Thakkar** and Sandeep Kumar), Sub- and Supercritical Hydrothermal Technology: Industrial Applications, 2019.
- Supercritical water gasification of biomass: Technology and challenges (**Anuj Thakkar** and Sandeep Kumar), Sub- and Supercritical Hydrothermal Technology: Industrial Applications, 2019.